BIOORTHOGONAL ANTIGENS ALLOW THE STUDY OF INTRACELLULAR PROCESSING AND PRESENTATION OF POST-TRANSLATIONALLY MODIFIED ANTIGENS

Can Araman[1,*], Linda Pieper-Pournara[1,*], Arieke S. B. Kampstra[2], Mikkel H. S. Marqvorsen[1], Clarissa R. Nascimento[1], Willemijn van der Wulp[3], G. J. Mirjam Groenewold[1], Marcel G.M. Camps[4], Ferry A. Ossendorp[4], René E. M. Toes[2,⇑] and Sander I. van Kasteren[1,⇑]

[1]Department of Bio-organic Synthesis and Institute of Chemical Immunology, Leiden Institute of Chemistry, Leiden University, Leiden, The Netherlands

[2]Department of Rheumatology, Leiden University Medical Center, Leiden, The Netherlands

[3]Department of Cell and Chemical Biology, Leiden University Medical Center, Leiden, the Netherlands.

[4]Department of Immunohematology & Blood Transfusion, Leiden University Medical Center, Leiden, The Netherlands

[*]: These authors contributed equally to this work

[⇑]: Correspondence to: Sander I. van Kasteren: s.i.van.kasteren@chem.leidenuniv.nl

Rene E. M. Toes: r.e.m.toes@lumc.nl

Abstract

Post-translational modifications (PTMs) have been implicated in several (auto)immune diseases. For example, citrullinated and carbamylated self-proteins are targeted by the auto-immune response in Rheumatoid Arthritis (RA). At present, little is known on the processes leading to autoimmunity. This is in part due to a lack of tools to image and assess the impact of these PTMs in antigen processing and presentation in antigen presenting cells (APCs).

Here we present a bioorthogonal chemistry-based approach by which biologically inert chemical handles are introduced into protein antigens, RA-autoantigen Vinculin$_{453\text{-}724}$ and the model antigen Ovalbumin, during expression, followed by the ligation of a fluorophore after uptake and processing in APCs via copper-catalyzed-azide-alkyne-cycloaddition (CuAAC). Using these "bioorthogonal antigens", individual effects of citrullination and carbamylation on antigen processing/presentation were investigated showing that for the RA-autoantigen vinculin, carbamylation, but not citrullination, increases antigen persistence in DCs. Neither of these modifications, however, translate to alterations in the activation of an anti-vinculin T-cell by human APCs.

Introduction:

Rheumatoid arthritis (RA) is a chronic inflammatory autoimmune disease affecting synovial joints. During the pathogenesis of this disease, T- and B-cell responses to post-translationally modified proteins are thought to lead to the emergence of full blown RA pathophysiology (Firestein and McInnes, 2017; Kokkonen et al., 2011). Two major post-translational modifications (PTMs) have been implicated in this immunopathogenesis: citrullination and carbamylation (Pruijn, 2015; Trouw et al., 2017; van Venrooij et al., 2011). Indeed, mature (IgG) anti-citrullinated protein autoantibodies (ACPAs) are found in 60-70% of RA patients, even before the onset of RA (Firestein and McInnes, 2017). The auto-immune response

against these post-translationally modified antigens is hypothesized to play a role in disease pathogenesis and is therefore subject of intense study (Rantapää-Dahlqvist et al., 2003; Scherer et al., 2018; van der Woude and Catrina, 2015).

Citrullination (**Fig. 1A and Scheme 1, lower panel**) is the enzymatic deimination of arginine by peptidyl arginine deiminases (PADs) (Baka et al., 2012; Fearon, 1939; Vossenaar et al., 2003), which may occur under non-inflammatory conditions (György et al., 2006). Under inflammatory conditions, the extensive citrullination by upregulated PAD-enzymes of self-proteins, such as vimentin (Bang et al., 2007), fibrinogen (Blachère et al., 2017; Vander Cruyssen et al., 2006), histones, and vinculin (Kampstra and Toes, 2017; van Beers et al., 2013; van Heemst et al., 2015), has been reported. These modified proteins have been shown to be recognized by the immune system and thought to give rise to arthritic symptoms in RA (Ali and Vino, 2016; Snijders et al., 2001; Titcombe et al., 2018).

Carbamylation, in contrast to citrullination, is a non-enzymatic PTM of the ε-NH_2 group of lysine. The reaction of this amine with free cyanate results in the formation of an ureido-group (**Fig. 1A and Scheme 1, upper panel**). This cyanate is in turn produced by the spontaneous dissociation of urea (Stark et al., 1960) or via myeloperoxidase-catalyzed conversion of thiocyanate during the neutrophil-mediated immune response (van Dalen et al., 1997). Structurally, the resulting product homocitrulline, is the one -CH_2 extended analogue of citrulline. This modification too has been implicated in RA immunopathogenesis. Indeed, autoantibodies against carbamylated proteins (anti-carbamylated protein antibodies, ACarPAs) have been discovered in sera of about 50-60% of RA-patients (Shi et al., 2011) and partial cross-reactivity has been reported between ACPAs and ACarPAs (Jiang et al., 2014; Truchetet et al., 2017).

ACPAs and ACarPAs are often found with matured (IgG) heavy chains (Fazilleau et al., 2009) pointing to T-cell involvement in their generation (Mydel et al., 2010). This indicates

that neo-epitopes not presented in the thymus are likely presented to naïve T-cells and presented in a pro-inflammatory context to activate the ($CD4^+$) T-helper cells.

There are two putative mechanisms by which these modifications can result in presentation of neoantigens to T-helper cells. The first of these is direct presentation of citrullinated/carbamylated epitopes by MHC-II molecules. Evidence in support comes from studies on genetic predisposition to RA: the most prominent genetic risk factor for developing $ACPA^+$ RA is found in the Human Leukocyte Antigen (HLA) haplotypes containing the Q/R-K/R-R-A-A binding pocket, also known as the shared epitope sequence (e.g. HLA-DRB1*04:01 (MacGregor et al., 1995)). This sequence lines one of the peptide binding pockets in the β-chains of these major histocompatibility complex (MHCs)-molecules and - by virtue of its positive charge - has an affinity for negatively charged or neutral amino acids, but not for positively charged amino acids. Cairns and co-workers have shown that the conversion of an arginine (cationic) into a citrulline (neutral) can drastically alter the affinity for peptides in their binding to these HLA-molecules, conceivably explaining how T-cell help can be induced by the alteration from Arg→Cit (Hill et al., 2003; Scally et al., 2013).

A second effect of citrullination and carbamylation could be beyond the direct alteration of epitope production during proteolysis. Changes in the charge (and thereby structure) of the protein could result in altered proteolysis and thus in the presentation of, otherwise, cryptic epitopes (Moudgil and Sercarz, 1994). As citrullination likely does not take place in the thymus during T-cell selection, these peptides will be new to the immune system, indicating that T-cells specific for these non-mutated *neo*-epitopes are not tolerized (Sercarz et al., 1993).

It is difficult to study the change in proteolytic susceptibility of antigens, especially within live cells or organisms. The go-to approach for studying antigen processing has been either the use of model proteins (Cebrian et al., 2011; Giodini and Cresswell, 2008; Norbury et al.,

1997) or the use of fluorophore-modified antigens (Princiotta et al., 2003; Rostovtsev et al., 2002; van Montfoort et al., 2009; Zaidi et al., 2007). However, when studying the degradative interaction of a specific protein, these approaches have several limitations. For example, model antigens or fusion to detectable polypeptide tags are only visible until they are degraded by proteolysis (van Elsland et al., 2016), which means – as proteolysis is essential for the liberation of epitopes for MHC-II loading – that they cannot be visible throughout the whole processing pathway (van Kasteren and Overkleeft, 2014).

Small molecule fluorophores (that are not proteolytically degraded) offer an alternative strategy. Their low molecular weight (~ 800 Da) is advantageous and they are usually introduced to ε-amine side chain of lysine residues of a protein. However, the fact they are aromatic, hydrophobic groups – often also charged – and that multiple copies are introduced into the protein to facilitate detection can alter the physical properties of the protein antigen (Pickering and Davies, 2012; Voss et al., 1996). Their appendage from lysine residues by means of an amide condensation reaction also renders them unsuitable for the study of lysine-PTMs, such as carbamylation. Alternative methods are thus needed to study processing of these PTM-modified autoantigens.

Here we describe an alternative strategy to study the effect of protein carbamylation and citrullination on antigen proteolysis to visualize the antigen (and its breakdown products) inside an APC without affecting processing and presentation, one based on bioorthogonal chemistry (Sletten and Bertozzi, 2009).

Bioorthogonal chemistry is the performance of a selective chemical ligation reaction in the context of the biological milieu (Qin et al., 2018; Ramil and Lin, 2013). A small abiotic group, such as an azide or alkyne is first introduced into a biomolecule or class of biomolecules and this functional group can then – when the biological time course is completed – be selectively modified with a detectable group (e.g. fluorophores or biotin) for

identification. The key feature of the approach is that – in an ideal scenario - neither the small handle nor the chemical functionality used to attach the detectable group react with other chemical groups present in the biological sample, but only with each other. The first example of these was the Staudinger-Bertozzi ligation (Saxon and Bertozzi, 2000), and many other reactions have been developed since (Lang and Chin, 2014), that even allow – under certain conditions –the performance of the ligation reaction in mice (J Exp MedNat Rev RheumatolChang et al., 2010). One reaction that we have used often is the copper-catalyzed [3+2] azide-alkyne cycloaddition (CuAAC) (Rostovtsev et al., 2002; Tornøe et al., 2002). For the study of the endolysosomal environment this reaction – although not readily compatible with live cell labeling – is optimal as the reaction partners are not only bioorthogonal in their reactivity, they are also fully stable to the conditions found during endo/phagosomal maturation (Bakkum et al., 2018). Recombinant proteins lend themselves very well to modification with the reaction handles for the CuAAC (**Fig. 1A**) (Kiick et al., 2002a): using the reported promiscuity of the methionine (Met) tRNA and tRNA-synthase (Kiick and Tirrell, 2000; van Hest et al., 2000) – especially when using expression strains auxotrophic for methionine – multiple copies of bioorthogonal amino acids, such as azidohomoalanine (**Aha, Fig. 1B**), or homopropargylglycine (**Hpg**, **Fig. 1B)** can be incorporated into the protein backbone in place of methionine yielding recombinant proteins in which (nearly) all Met loci are replaced with a click-handle. Using this approach, for example, the TIM-barrel protein beta-galactosidase from *Sulfolobus solfataricus*, could be produced without loss of catalytic activity, and subsequently decorated with different moieties, e.g. glycans, using a CuAAC chemistry (van Kasteren et al., 2007b).

For studying the *in cellulo* degradation of antigens, we envisioned that these bioorthogonal proteins containing multiple bioorthogonal groups (as opposed to single modifications that can be introduced using e.g. amber codon suppression (Wals and Ovaa, 2014)) would allow

us to follow degradation, as the modifications are small and very similar to the wildtype Met-residue (Sletten and Bertozzi, 2009), stable under physiological conditions (Bakkum et al., 2018) and – most importantly for studying carbamylation of antigens – do not compete with lysine PTMs for occupancy as conventional fluorophore modification does (**Fig. 1A**).

This bioorthogonal approach would thus allow the unbiased reporting of the degradation of antigen inside APCs, while simultaneously studying the eventual presentation of the antigen. Here, we describe the optimization of these 'bioorthogonal antigens' and their application to the study of citrullinated and carbamylated antigens.

Results:

We initially used fluorophore-modified antigens to study uptake, processing and presentation (Fig. 1C). However, MHC-II-restricted presentation (by murine dendritic cells derived from bone marrow (BMDC)) to $CD4^+$ T-cells isolated from an B6.Cg-Tg(TCRαTCRβ)425Cbn/J (OT-II)-mouse, specific for the ovalbumin peptide 323-339 (ISQAVHAAHAEINEAGR) (Barnden et al., 1998a), showed a >10-fold increase from (Alexa-647-lysine)-modified Ova, Alexa-647 Ova, compared to the unmodified antigen (**Fig. 1C**). This significantly altered antigen-presentation is likely due to changes in physical properties of Alexa-647 Ova. In light of these data, and due to our interest in carbamylation of antigens and the competition for lysine occupancy between carbamylation and the fluorophores, we abandoned the use of fluorophore modified antigens for the study of carbamylation and citrullination on antigen processing.

Bioorthogonal antigens

We instead opted to produce bioorthogonally labelled variants of both the model antigen ovalbumin (Ova) and the RA-autoantigen vinculin (Vin) (van Heemst et al., 2015). To

incorporate the bioorthogonal groups into these antigens, we employed the methionine auxotrophic strain B834 of *E. coli* (Wood, 1966). This *E. coli* strain, by virtue of its inability to synthesize methionine, can incorporate unnatural amino acids that are substrates of methionine aminoacyl tRNA synthetase in an efficient manner. This technique is, for example, commonly exploited to produce selenomethionine containing proteins (Leahy et al., 1992), and was used by Tirrel and colleagues to produce proteins with bioorthogonal and other unnatural chemical functionalities (Kiick et al., 2002a; Kiick and Tirrell, 2000; Kiick et al., 2001; van Hest et al., 2000). The approach is straightforward: a simple addition of the required Met-analogue to a Met-free growth medium is the only requirement. The approach affords quantitative incorporation efficiencies (van Kasteren et al., 2007b). We chose to introduce Aha (Kiick et al., 2002a) and Hpg (Kiick et al., 2001) as the bioorthogonal amino acid analogues. The chemical functionalities of these amino acids (azide and alkyne) are biologically stable, (Bakkum et al., 2018; Laconte et al., 2005; van Geel et al., 2012) and very small (2-3 atoms). We hypothesized that these properties would give us the highest chance of obtaining a protein with a similar structure and similar antigenic properties to the non-bioorthogonal variant. In addition, a protein antigen containing multiple copies of the bioorthogonally reactive chemical handle would allow the imaging of multiple fragments during degradation.

At the same time, the azide and alkyne also give the most extensive options with respect to available bioorthogonal ligation reactions (Lang and Chin, 2014). The expression of the protein does have to be performed in *E. coli,* meaning that the proteins are expressed without glycans. This does reduce heterogeneity and potentially complicating effects of glycans on antigen processing (Burgdorf et al., 2007; Burgdorf et al., 2010).

We thus set out to synthesize carbamylated and/or citrullinated bioorthogonal antigens using the methionine replacement-approach. To study the processing of antigens by APCs during

RA, we chose to produce a truncated vinculin (Vin) variant bearing the immunoactive DERAA motif comprising aa 453-724 of the native Vin sequence as a T-cell receptor against this epitope was available. This protein was fused to an N-terminal Deca-His-Tag (His_{10}) *via* an Enterokinase cleavage site (DDDDDKH). The immunoactive peptide recognized by self-reactive Vin-directed T-cells contains an Arg (R), and hence can be modified by citrullination. Therefore, care as to be taken, when studying the ultimate presentation to T-cells later on, when studying the ultimate presentation to T-cells later on, as citrullination could affect T-cell activation of a the DERAA-containing epitopes and the removal of charge from an epitope can eliminate T-cell recognition, even with equal MHC-loading (Huse et al., 2007; Pawlak et al., 2015; van der Gracht et al., 2018). Therefore, we also produced Ova from the plasmid pMCSG27 (containing Ova fused to a Hexa-His-Tag (His_6), *via* a TEV cleavage site; a kind gift from N. del Cid and M. Raghavan (Del Cid et al., 2012)).

The above genes for Vin and Ova were expressed in the Methionine auxotrophic *E. coli* (strain B834) (van Hest et al., 2000) using existing protocols (Kiick et al., 2002b; van Kasteren et al., 2007a). The proteins were expressed in good yields (8-15 mg/L culture after purification for Ova and Vin respectively), characterized via SDS-PAGE (**Fig. 2A for Vin, Fig. 2D for Ova**), circular dichroism (**CD, Figure 2C for Vin, Fig. 2F**) and liquid chromatography mass spectrometry (**LC-MS**, **Supplemental Fig. S1-2**). Mass spectrometric analysis confirmed the presence of bioorthogonal groups in both the Vin and Ova proteins (**Supplemental Fig. S1 -2**). Vinculin contains 8 methionine codons for incorporation (plus the Met-encoding start codon, which is usually cleaved off during expression (van Kasteren et al., 2007b)). For Vin, a mixture of proteins was obtained containing mainly 7 or 8 copies of Hpg or Aha. Minor variants (combined abundancy < 10% according to MS) with fewer (6, 5 and 4) copies of Aha and Hpg were also detected (**Supplemental Fig. S1 E-F**). For bioorthogonal

Ova variants, incorporation levels were all shown to be quantitative (**Supplemental Fig. S2 B-C**).

Aha- and Hpg-Vin/Ova can be citrullinated and carbamylated to the same extent as wt protein.

We next assessed whether the bioorthogonal antigens could be post-translationally modified the same way as wildtype (wt) proteins. All proteins were carbamylated and citrullinated as described (Chang et al., 2005; Fando and Grisolia, 1974). Carbamylation was performed using potassium cyanate (**Scheme 1, upper panel**) and the reaction completion was confirmed *via* SDS-PAGE as well as LC-MS measurements. All Vin variants used in this work contained 23 possible carbamylation sites (incl. the N-terminus). Results of SDS-PAGE and LC-MS measurements showed that >19 amines were carbamylated for all variants (**Fig. 2A-B**). Similar carbamylation levels were observed between the bioorthogonal and wt variants; with wt-Vin carrying 19 carbamyl moieties, Aha-Vin 20, and Hpg-Vin 19.

Ova variants contain 21 possible carbamylation positions. All bioorthogonal Ova variants could be carbamylated, as confirmed by SDS-PAGE (**Fig. 2D**), LC-MS (**Fig. 2E**) and further characterized by CD (**Fig. 2F**). The degree of carbamylation for the bioorthogonal Ova variants (wt: 21, Aha-Ova: 18 and Hpg-Ova: 21 carbamyl-groups) was similar to those of Vin.

In vitro citrullination was performed through utilization of recombinant human PAD4 (Sigma Aldrich, the Netherlands). There are 19 arginines present in wt-Vin. The quantity of Arg → Cit conversion was determined via LC-MS (**Supplemental Fig. S1**) and further analyzed via SDS-PAGE (**Fig. 2A**). The results indicated that all arginines were converted into citrullines in the wt, as well as in all of the bioorthogonal variants.

Citrullination and carbamylation alter protein structural stability

We next analyzed the effect of citrullination and carbamylation on the secondary structure of Vin by circular dichroism (Chang et al., 1978) (**Fig. 2C&F**).

Interestingly, we found that Aha-Vin and Hpg-Vin without modifications already show a more pronounced negative Cotton effect (minima at 210 and 222 nm, respectively), in comparison to the wt-Vin with similar α-helicity, indicating an increased rigidity in the structure.

Furthermore, carbamylation of all Vin variants increased rigidity significantly (~ 5-fold assessed via spectrum minima by similar helicity, **Fig. 2C**) when compared to their unmodified counterparts. In contrast, acetylated Vin derivatives – which were included as a control for non-carbamyl lysine capping – showed a decreased α-helical content (15.8% wt-Vin, 10.8% Aha-Vin and 25.7% Hpg-Vin, **Table 1**) with a pronounced shift towards a higher content in random coils (33.7% wt-Vin, 35.0% Aha-Vin and 29.3% Hpg-Vin, **Table 1**), suggesting the stabilization of the secondary structure induced by carbamylation is not due to the removal of the positive charges on lysines.

Citrullination of the Vin-derivatives had a different effect on the structure: these proteins became high in β-sheet content (48.9% wt-Vin, 52.7% Aha-Vin, 42.4% Hpg-Vin respectively) and random coil-rich structure with a decrease in the content of α-helices (**Table 1**). These results show that the PTMs of Vin cannot only alter its stability, but the actual fold of the protein as well. Also, the bioorthogonal variants – whilst showing quantitative differences compared to wildtype – followed the same trends.

The modification of the Ova-variants yielded more complex effects on protein structure: carbamylated wt-Ova had a higher α-helical content and adopted a slightly decreased random coiled structure when compared to its non-modified version (**Fig. 2F and Table 1**). Interestingly, upon carbamylation of Aha-Ova, the secondary structure did not change

significantly (19.9% to 19.8% α-helix content) (**Fig. 2F**). For Hpg-Ova, a significant increase in negative Cotton effect for α-helices (> 7% increase in α-helicity, **Table 1**) and a decrease in random coil content (~ 5% less random coil, **Table 1**) could be detected. Citrullinated wt-Ova showed a more pronounced negative Cotton effect compared to the bioorthogonal versions, but their percentage distribution of secondary structure elements remained the same as in non-modified versions, indicating a tightening of the structure.

Carbamylation slows down antigen degradation in vitro

We next studied the influence of the structural effect of carbamylation and citrullination on the degradation of the bioorthogonal antigens. For this purpose, lysosomes were isolated from the murine RAW 264.7 macrophage cell line (Walker and Lloyd–Evans, 2015). Reaction mixtures contained wt or bioorthogonal antigens (15 µM final concentration), isolated lysosomes (18 µg total amount of protein), with the pH adjusted to pH 5.0. Samples were taken at various time points (0, 30 min, 1h, 2h, 4h, 18h, 24h, and 48h). Carbamylated wt-, Aha- and Hpg-Vin (**Fig. 3**) showed a greater resistance to proteolysis than their non-modified counterparts. After 18h of incubation, all non-carbamylated Vin variants had been degraded > 50%, as determined by densitometry. wt-Vin and Aha-Vin showed a higher susceptibility to *in vitro* lysosomal degradation (>70% degradation) than Hpg-Vin (>50% degraded). Carbamylation of the Vin-variants decreased the susceptibility towards proteolysis (<10% degradation observed at t = 24 and 48 h for carbamylated Aha-Vin and Hpg-Vin and <30% for carbamylated wt-Vin). Citrullination of the antigens had no significant effects on the rate of degradation (**Supplemental Fig. S3 A-C**). Ova did not show any proteolytic degradation when incubated with lysosomes (**Supplemental Fig. S3 D**), in agreement with previously published results (Shen et al., 2004; T. et al., 2000; Trombetta et al., 2003). Thus, the effect of carbamylation and/or citrullination on antigen processing was not relevant for this antigen.

Taken together, the results presented here indicate that carbamylation alters not only the structure of the autoantigen Vin, but can also alter its resistance to lysosomal proteases *in vitro,* whereas alterations in protein structure upon citrullination do not cause any changes in its *in vitro* proteolytical stability using lysosomal extracts.

Carbamylated bioorthogonal antigens are processed more slowly by DCs

One advantage of bioorthogonal antigens is that their fate can be selectively followed even in cell lysates. Moreover, the chemical handles in the antigens could be specifically labelled with a sufficient signal-to-noise to allow their detection within the APC-proteome. To investigate whether citrullinated and carbamylated proteins are processed differentially by APCs than their non-modified counterparts, the rate of proteolysis of these autoantigens was determined in BMDCs (Inaba et al., 1992; West et al., 2004). BMDCs are adequate APCs to study the *in cellulo* aggregation of bioorthogonal antigens due to their lysosomal enzymatic content and acidic pH tolerance (Angew Chem Int Ed EnglProceedings of the National Academy of SciencesMartínez et al., 2007; Trombetta et al., 2003).

BMDCs were pulsed with the antigens for 1h. The cells were then chased for 1h, 24h or 48h prior to cell harvest, lysis followed by a CuAAC ligation with the appropriate fluorophore. The labelled lysates were then separated by SDS-PAGE and the signal stemming from the bioorthogonal groups measured using in-gel fluorescence **(Fig. 4 and Supplemental Fig. S4**). Wt-variants of the protein were not visible due to the absence of CuAAC reactive groups (representative results of wt-and carb_wt-Vin are shown in **Supplemental Fig. S4)**. Aha-Ova and Hpg-Ova, however, could be visualized in DCs at t = 1h, after incubation at a concentration of 4 μM (**Supplemental Fig. S4 D**). The same held for Aha-Vin and Hpg-Vin (**Fig. 4A**). At t = 24h none of the antigens (including ovalbumin; in striking contrast to the *in vitro* experiments with lysosomes) were visible anymore, suggesting complete degradation at

this timepoint. The same was observed for citrullinated variants (**Fig. 4B and Supplemental Fig. S 4E**) of both proteins. Carbamylated antigens on the other hand showed a clear signal at t = 24h for all antigens, with a detectable signal even observed at t = 48h for carbamylated Hpg-Vin (**Fig. 4 and Supplemental Fig. S4**).

Experiments with shorter chase periods for wt and citrullinated variants indicated that for both proteins all bioorthogonal bands >1 kDa disappeared between 2-3h. To determine whether the striking effect on in cell-stability resulting from carbamylation was a result of the specific modification, or simply because of the absence of amine/ammonium functionality on the protein, an acetylated variant of Vin was also analyzed. This protein too was degraded completely at t = 3h, indicating the observed stabilization effect is carbamylation-specific (**Supplemental Fig. S 4B**). These results indicate that carbamylation affects the rate of protein breakdown similar as found in the experiments using lysosomal extracts.

Moreover, it is demonstrated that, by using the bioorthogonal antigens, the fate of one specific antigen can be followed and visualized even in APCs, as the chemical handles in the antigen could be specifically labelled with a sufficient signal-to-noise to allow their detection within the APC-proteome. Furthermore, this methodology does not disturb the uptake of the antigen, thus approximating the natural biological process more closely than what has been possible hitherto.

Unmodified, carbamylated and citrullinated bioorthogonal antigens are equally presented to T-cells.

To determine whether the increased resistance to proteolytic degradation upon carbamylation translated to an alteration in antigen presentation, we assessed the ability of the Ova-variants to activate OT-II (CD4+) T-cells in co-culture with murine BMDCs. Bioorthogonal modification did not affect antigen presentation significantly (**Fig. 5A**), confirming the

suitability of these reagents for antigen presentation studies. For Ova, no significant alteration of T-cell proliferation assessed by the IL-2 production was observed upon carbamylation (**Fig. 5B-D**).

Although the studies with Ova and murine immune cells are important for highlighting the suitability of our bioorthogonal approach, we aimed to use human cells to address the question whether the approach can be used in an actual human disease model. Specifically, to investigate the influence of PTMs on the presentation and recognition of the RA-antigen Vinculin, we transduced the Jurkat T-cell line (J76) with a T-cell receptor (TCR) restricted to a specific peptide present in vinculin (REEVFDERAANFENH; VCL-DERAA) as described (Rosskopf et al., 2018). To date, transgenic lymphocytes expressing the TCR specific for vinculin epitopes are not available. The J76 subline is devoid of endogenous TCR alpha and beta chains, circumventing the problem of TCR miss-pairing and unexpected specificities (Rosskopf et al., 2018). The resultant reporter cells allow simultaneous determination of the activity of the transcription factors NF-κB, NFAT and AP-1 that play key roles in T-cell activation. The percentage of fluorescence positive cells after antigen-specific activation can be readily measured using flow cytometry.

The Jurkat-DERAA cells were first stimulated by a HLA-DQA1*03:01/DQB1*03:02+ (HLA-DQ8+) EBV-transformed B cell line loaded with titrated amounts of the vinculin peptide recognized by the TCR. The Jurkat T-cells showed a peptide dose-dependent response as determined by eCFP expression as read-out (**Fig. 6A-B**). The response was HLA-DQ8-restricted as HLA-DQ8-negative B cells were unable to stimulate the Jurkat T-cells (**Supplemental Fig. S5**). Next the monocyte-derived dendritic cells, isolated from HLA-DQ8+ donors, were pulsed o.n. with different bioorthogonal proteins and their modified counterparts (3 µM). After DC maturation for 30 hrs, the Jurkat T-cells were added and used as read-out for HLA-restricted T-cell activation by flow cytometry (**Fig. 7 and Supplemental**

Fig. S5). As for the ovalbumin antigens, no differences were observed between carbamylated and wildtype antigens, whereas bioorthogonal antigens again behaved the same as their wildtype counterparts (**Fig. 7C-D**). Citrullinated Vin variants showed a reduced T-cell activation, likely due to citrullination within the DERAA-containing epitope blocking the epitope for recognition by the TCR (**Fig. 7**).

DISCUSSION

Since its inception at the turn of the millennium, bioorthogonal ligation chemistry has rapidly become a stalwart for the detection of otherwise undetectable biological groups (Sletten and Bertozzi, 2009). Its application to the imaging of lipids (Hang et al., 2011), glycans (Saxon and Bertozzi, 2000), nucleic acids (Buck et al., 2008), peptidoglycan (Siegrist et al., 2012), and proteins (Kiick et al., 2002a) has greatly assisted the understanding of the biology of these – often otherwise invisible – biomolecules. In this paper we have applied the approach to a new class of undetectable events, namely keeping antigens visible during their proteolytic degradation; something that is not possible with protein or peptide-based labelling methods such as fluorescent proteins (van Elsland et al., 2016), as such labels are destroyed by the very same proteases that liberate MHC-II and its binding peptides (van Kasteren and Overkleeft, 2014).

As shown in Figure 1, the current best approach for imaging using fluorophore modified antigens increases IL-2 production over 10-fold, rendering observations regarding processing of these epitopes questionable in their relevance. The expression of proteins with the methionines replaced for the non-canonical analogues Aha and Hpg – two amino acids that are reactive in multiple bioorthogonal ligation chemistries (Lang and Chin, 2014) – as described here improves on this. The structure of the proteins is minimally altered upon modification and the rates of proteolysis are also similar *in vitro* and in intact T-cells. T-cell

activation by all species also remains the same, although in situations where PTMs could display different antigenicity, we may also observe differences between bioorthogonal and wildtype antigens.

An additional feature of the bioorthogonal antigens described in this paper is that they are introduced within the sidechain of methionines, rather than lysines when fluorophores are appended from a protein. We exploited this feature to study the effect of lysine carbamylation on antigen processing and presentation, as these modifications appear to play a role in disease pathogenesis of RA. For example, carbamylation of lysine residues on e.g. Fibrinogen has been found to be implicated in RA and carbamylated proteins are readily recognized by autoantibodies (Jones et al., 2017). Moreover, it has also been shown that fibroblast-like synoviocytes can generate carbamylated proteins upon autophagy of self-proteins (Manganelli et al., 2018). Like the closely related modification, citrullination, modified proteins are found in the synovial joints of RA patients, and additionally can be recognized by ACPAs and ACarPAs. As has been previously described by Van Heemst *et al*, vinculin carries a particular sequence, the DERAA sequence, which is possibly involved in the development of seropositive RA disease (van Heemst et al., 2015). Here, we show that the DERAA-epitope cannot only be processed from vinculin and presented to T-cells, but also that carbamylation of Vinculin affects its stability and susceptibility to degradation. In addition, carbamylation of lysine residues resulted in increased secondary structure stability (**Fig. 2C**). Likewise, citrullination of Vin yielded a complete change of the secondary structure towards β-sheets and random coils (**Fig. 2C**). This is not entirely unexpected, since the effects of citrullination on protein secondary and tertiary structure have been reported, although still controversial. For example, proteins such as the extracellular matrix protein Tenascin C does not exhibit any conformational changes (Schwenzer et al., 2016) whereas trichohyalin (Tarcsa et al., 1996) or HSP90 (Travers et al., 2016) have been reported to undergo a complete unfolding upon

citrullination. Taken together, these results indicate that citrullination is a PTM with a complex nature and more insights into structural elements of citrullinated proteins should be provided.

The J76 T-cell line is a powerful tool to demonstrate that RA-related biorthogonal antigens are presented at the same levels as wildtype antigens. Unfortunately, we could not determine the effect of citrullination on antigen-presentation to T-cells as the Arg (R) in the epitope from Vinculin recognized by the TCR in the reporter Jurkat T-cell line became citrullinated. Due to this citrullination, the TCR could not recognize the epitope anymore explaining the reduced T-cell activation of the citrullinated vinculin variant.

Carbamylation clearly affected protein degradation *in vitro* by lysosomal extracts, indicating that carbamylation modulates protein stability. Indeed, these observations were paralleled by the findings made using dendritic cells showing that carbamylated proteins are more stable as compared to their unmodified counterparts. The notion that carbamylated proteins display an increased stability and are more resistant to proteolytical activity could have important consequences for the recognition by immune cells and antibodies as it is conceivable that more stable proteins will be exposed for a prolonged time to the immune system, thereby influencing its ability to serve as a target for immune recognition. The latter is not only relevant for the recognition by autoantibodies, but possibly also for the recognition and/or activation, respectively tolerance induction of T-cells. Therefore, it was unexpected to find that carbamylation of neither Ova nor Vin seemed to alter the strength of the CD4-restricted T-cell response in our assays. The reason why these differences in protein stability is not reflected in differences in T-cell activation is not known but could be related to the notion that once a certain threshold of antigen-levels is reached, T-cell activation is not affected anymore. We did not study whether the enhanced stability of carbamylated proteins will lead to a prolonged antigen-presentation to T-cells. The latter would be relevant to study in further

studies as it is conceivable that prolonged antigen-presentation will affect T-cell activation and/or tolerization. Likewise, the second aspect that merits further investigation is not whether the absolute presentation of dominant antigens is altered, but whether the repertoire of peptides changes upon citrullination, which can be investigated by mass spectrometry among many other techniques, as this would lend credence to the hypothesis that the changes in proteolytic susceptibility would lead to the presentation of neo-epitopes (Castellino et al., 1998; Moss et al., 2007; Stern et al., 1994; Unanue et al., 2016).

In summary, we were able to show that our bioorthogonal antigen variants are powerful tools to give more insights into the immunopathogenesis of autoimmune diseases such as RA. It was shown that bioorthogonal antigens can be taken up and processed as their wt counterparts but enable the visualization of intracellular processing better than most of the fluorophore-labeled, commercially available antigens. Furthermore, these results suggest that depending on the type of PTM (e.g. citrullination and carbamylation) and the nature of the protein, protein processing and presentation is influenced differently, conceivably leading to alterations in immune response. Thus, we were able to develop a specific method for recognition of RA-related and discrimination of non-RA related (i.e. non-modified) autoantigens. Our future work will focus on the site-specific introduction of citrullination and carbamylation into Vin and other autoimmunity related proteins in order to assess site-specific and individual effects of these PTMs in health and disease.

Materials and Methods:

Chemicals

Chemical reagents for buffer preparation and chemical synthesis were purchased from Acros (Belgium), Chem-Lab (Belgium), Honeywell Riedel-de Haën (Germany), Merck (The Netherlands), Novabiochem (The Netherlands), Sigma Aldrich (The Netherlands), Sigma Life Sciences (The Netherlands) or Sphaero Hispanagar (Spain) and used without further purification unless stated otherwise.

Fluorophores (Alexa Fluor 488 Azide, Alexa Fluor 488 Alkyne, Alexa Fluor 647 Azide and alkyne), were purchased from Thermo Fisher Scientific.

Cell Culture

Bone Marrow Dendritic Cell Differentiation

Bone marrow (BM) was isolated from 8-12 weeks old C57BL/6 mice kept under specific pathogen-free conditions (Strain: C57Bl/6NHsd, H-2^b Haplotype; Envigo Inc., Huntingdon, United Kingdom) essentially as described (Hoogendoorn et al., 2014; Lutz et al., 1999). Femurs and tibiae of female or male mice were removed and surrounding tissue was removed. Thereafter, intact bones were left in 70% ethanol for 2–5 min and washed with sterile PBS. The bone marrow was flushed from femurs and tibia after removal of the bone-ends using pre-warmed IMDM (Sigma, ref# I3390) using a 20 mL Syringe with a 0.45 mm x 23 mm hypodermic needle (G26, Terumo Europe, NN-2623R). The BM was then homogenized through a 70 µm cell strainer (Falcon, ref# 352350).

The cells were then centrifuged 5 min at 350 *g* and resuspended in 10 mL IMDM supplemented with 8% heat-inactivated fetal calf serum (FCS, Sigma, ref# F0804, lot# 015M3344), 2 mM Glutamax^{TM} (GIBCO, ref# 35050-038), 20 µM 2-Mercaptoethanol (Gibco, ref# 31350010), 50 IU/mL penicillin and 50 µg/mL streptomycin, and recombinant GM-CSF (20 ng/mL, Peprotech, ref# 315-03) to a concentration of $0.5x10^6$ cells/mL. The cells were incubated in non-adhesive petri dishes at 37°C, 5% CO_2, under humidified air.

OT-II isolation and Culturing

OT-II mice (CD4+ T-cell transgenic mice expressing a TCR recognizing the OVA-derived T_h epitope ISQAVHAAHAEINEAGR in association with I-Ab) (Barnden et al., 1998b) were bred and kept at the Leiden University Medical Center animal facility as well as at the Leiden Advanced Drug Research Centre (kindly provided by Dr. Bram Slutter) under specific pathogen-free conditions. All mice were used at 8–12 wk of age (Ho et al., 2017).

Briefly, spleens from OT-II TCR transgenic mice were harvested and homogenized using a 70 µm cell strainer. Untouched CD4+ T-cells were isolated with a Milteny mouse T-cells isolation kit for CD4+ T-cell negative selection, according to the manufacturer's instructions. CD4+ T-cells purity was typically higher than 85%.

Human Cell Culture Protocols

Dendritic cell generation

HLA-DRB1*04:01/-DQA1*03:01/-DQB1*03:02 (HLA-DR4/-DQ8)-positive buffy coats were received from Sanquin Bloodbank. Peripheral Blood Mononuclear Cells (PBMCs) were isolated with Ficoll-paque gradient and CD14+ cell isolation was performed with MACS beads according to the manufacturers protocol with slight alterations (Cat#: 130-097-052, Miltenyi Biotec). In short, PBMCs were incubated with $10uL/10^7$ cells $CD14^+$ microbeads and incubated for 15' at 4°C. Coated PBMCs were run over an LS column twice to purify the $CD14^+$ fraction. To differentiate the $CD14^+$ cells to dendritic cells, the $CD14^+$ cells were counted and seeded at $5x10^5$ cells/well in a 24-wells plate, in medium (IMDM, Cat#:12440-053, Gibco) supplemented with 1% Glutamax, 1% Penicillin/streptomycin, 8% Fetal Calf Serum (FCS), 800 U/mL GM-CSF (Cat#:300-03, Peprotech) and 500 U/mL IL-4 (Cat#:200-04, Peprotech) and cultured for 6 days. After differentiation of the $CD14^+$ cells to immature dendritic cells, the cells were fed with 200 µg POI per well and were allowed to take it up for ~18 hours. Peptides were added 1 hour before maturation at 10µg/mL.

Subsequently, the dendritic cells were matured with a maturation cocktail: 100 ng/mL GM-CSF (Cat#: 300-03, Peprotech), 15 ng/mL TNFα (Cat#: 210-TA-005, R&D), 10 ng/mL IL-1β (Cat#: 201-LB-005, R&D), 10 ng/mL IL-6 (Cat#:200-06, Peprotech), 1 µg/mL PGE2 (Cat#: 14010, Cayman Chemical), 500 U/mL IFNγ (Cat#: 300-02, Peprotech). Dendritic cells were allowed to mature for ~30 hours before they were harvested and co-cultured with the T-cells.

Jurkat Triple Parameter Reporter (TPR) cell line

A Jurkat 76 cell line, positive for CD4 (by transduction) and NFAT-eGFP, NFkB-CFP and AP-1-mCherry (by transduction) (Jutz et al., 2016; Rosskopf et al., 2018) was kindly provided by Mirjam Heemskerk from the LUMC. The cell line was transduced with Vin-DERAA-specific T-cell receptor in the group of Heemskerk by R. Hagedoorn, as has been previously

described (Rosskopf et al., 2018). The transduced Jurkat T-cells were selected on their TCR expression and sorted in single cells. One of these clones was shown to be highly responsive and was used for all future experiments described here. The JurkaT-cells are cultured in IMDM supplemented with 1% glutamax, 1% Penicillin/streptomycin and 8% FCS.

Recombinant protein expression

Vinculin

The plasmid (pET3d, Amp^R, Novagen) encoding of wild type $Vinculin_{435-742}$ (hereafter referred to as wt-Vin) was transformed into the methionine auxotroph *E.coli* B834(DE3) (met-aux, Genotype: F- ompT hsdSB (rB- mB-) gal dcm met(DE3), Novagen #ref 69041). The protein was expressed from the overnight culture of a single colony. 100 mL of this overnight culture (o.n., Ampicillin 50 µg/mL, 18 h, 37°C, and 150 rpm) was used for the inoculation per 1 L LB medium (Ampicillin 50 µg/mL, 37°C, 150 rpm). The cells were grown to an OD_{600nm} of 0.6-1.0 prior to the addition of 1 mM isopropyl-β-D-1-thiogalactopyranoside (IPTG) for 18 h (30°, 150 rpm). The cells were harvested by centrifugation (4000 g, 20 min, 4°C), washed once with Tris-buffered saline (TBS; 50 mM Tris-HCl, 300 mM NaCl, pH 8.0) and stored at -80°C for further use, if not used directly.

Cell lysis and affinity purification of $Vinculin_{435-743}$:

Cell pellets were weighed, resuspended in TBS to 1-4 g/mL, prior to lysis by French Press (1.8-1.9 kbar, Stansted, Pressure Cell Homogeniser). Lysed cells were centrifuged (15,000 *g*, 1 h, 4°C). The soluble fraction was then loaded onto a Ni-NTA affinity resin (Thermo Fisher Scientific, catalogue no. 88221) pre-equilibrated with TBS. After incubation for 1 h under gentle rotation, the beads were first washed with 2 column volumes (CV) of washing buffer 1 (TBS, 10 mM Imidazole, pH 8.0) and subsequently with 3 CV washing buffer 2 (TBS with 50 mM Imidazole). The resin was then treated with elution buffer (TBS, 250 mM Imidazole, pH 8.0, 2 mL) to obtain the protein of interest (POI) in ~ 10 mg/mL, which was then exchanged into TBS using a Sephadex G25 resin (PD-10 column; GE Healthcare). Purity of the POI was then determined using SDS-PAGE.

Expression of bioorthogonal vinculin variants

A single colony of *E. coli* B834 transformed with pET3d-Vin was grown in 50 mL LB augmented with 1% w/v glucose and grown overnight. The next morning, the culture was diluted 1:100 with fresh LB media and cells were grown to an OD_{600nm} of 0.5-0.6. The resulting culture was then centrifuged (2000 *g*, 10 min, 4°C) and the supernatant discarded. The cells were washed and resuspended in SelenoMet™ media (Molecular Dimensions, USA) without additional methionine. The cells were incubated at 30°C for 30 min, followed by 30 minutes at 37°C (180 rpm) after which either $_L$-Azidohomoalanine (Aha, 0.4 mM final concentration) or $_{D,L}$-Homopropargylglycine (Hpg, 0.8 mM final concentration) was added. The cells were incubated for a further 30 minutes at 37°C (OD_{600nm} 0.7-1), the culture was induced with 1 mM IPTG for 18 h. Cell lysis and purification were then performed as described above.

Incorporation efficiency of the bioorthogonal amino acids was analyzed by LC-MS and in-gel fluorescence using bioorthogonal ligation with appropriately modified (i.e. Azide/Alkyne) Cy5 and Alexa 488 dyes.

Ovalbumin expression

The gene for the wt, full length Ovalbumin (hereafter referred to as wt-OVA, accession number V00383) was cloned into the pMCSG7 vector as described elsewhere (Del Cid et al., 2012; Zhang et al., 2010) and transformed into the methionine auxotroph expression strain, namely *E.coli* B834(DE3). The construct contained an N-terminal M<u>HHHHHH</u>SSGVDLGT***ENLYFG***SNA sequence for Ni-NTA purification (underlined) and TEV-cleavage (italic bold). The expression was performed as described for wt-Vinculin.

Cell Lysis and purification of OVA

After the expression period, the cells were harvested by centrifugation (20 min, 3000 *g*). The pellet was resuspended in lysis buffer (50 mM NaH_2PO_4, 300 mM NaCl, 10 mM imidazole, pH 8.0, 10 % glycerol, 1 mg/mL Lysozyme (Amresco, ref#0663-5G), complete EDTA-free protease inhibitor (Roche, ref# 11836170001), β-mercaptoethanol (final concentration 5 mM), 250 U benzonase per 100 mL culture volume) to a final concentration of 5-10 g/mL. The cells were lysed with a French press at 1.9 kbar and the flow-through was centrifuged at 15,000 g (30 min, 4°C) to separate soluble and insoluble components. The soluble-fraction was purified using nickel-affinity chromatography using a fast protein liquid chromatography (FPLC) system (Äkta Start Purification System, The Netherlands). The soluble-fraction was loaded onto a Ni-NTA Superflow cartage (Qiagen, ref # 30721) that was equilibrated with 10 CV buffer 1 (50 mM NaH_2PO_4, 300 mM NaCl, 10 mM imidazole, 10% glycerol, pH 8.0). The column was washed with buffer 2 (10 CV, 50 mM NaH_2PO_4, 300 mM NaCl, 20 mM imidazole, 10 % glycerol, pH 8.0). Protein elution was then initiated by buffer 3 (50 mM NaH_2PO_4, 300 mM NaCl, 500 mM imidazole, 10 % glycerol, pH 8.0) using a 20% CV gradient (1 mL/min, 20 mL total volume), from 20 mM

up to 250 mM imidazole (50% Buffer 3). All fractions were analyzed via SDS-PAGE and fractions containing >90% ovalbumin were collected and combined.

The protein was further purified by anion exchange chromatography. The combined fractions were dialyzed overnight into binding buffer (50 mM NaH_2PO_4, pH 8.0) and loaded onto an anion exchange column (GE Healthcare-HiTrap Q HP, ref# 17-1153-01) that had been equilibrated with 10 CV binding buffer. The protein was eluted using an elution buffer gradient (50 mM NaH_2PO_4, 0-500 mM NaCl, pH 8.0). Elution fractions were analyzed by SDS-PAGE and the fractions containing the POI. were combined and dialyzed o.n. into 10-100 mM NaH_2CO_3, pH 8.0 to yield 2 mL of a 2-5 mg/mL solution of wt-OVA (yield 4-10 mg/L culture). The protein solution was snap-frozen and stored at -80°C until further use.

Expression of bioorthogonal OVA variants

Bioorthogonal protein expression was performed as described for the wt-OVA protein with the following changes. After reaching the optimal optical density of 0.6-0.9 for the pre-culture, the medium was exchanged for a methionine deficient medium (Molecular Dimensions, ref# MD12-501 and MD12-502) and the culture was left to grow for another 30 min at 37°C. Then the medium was supplemented with unnatural amino acid, namely, Aha (0.4 mM) or D-/L- Hpg (0.8 mM) and expression was induced by addition of 1 mM IPTG. Expression was continued o.n. (30°C, 180 rpm). The culture was harvested by centrifugation (30 min, 4 °C and 4000 g). The cells were lysed as above and purified as described for wt-OVA.

Enzymatic and Chemical Modification of Recombinant Proteins

In vitro Acetylation of Recombinant Proteins

Acetylation of recombinant Vin and OVA variants was performed as described elsewhere (Guan et al., 2010).

In vitro Carbamylation of recombinant proteins

Vin and OVA variants were carbamylated using a protocol adapted from Fando *et al.* (Fando and Grisolia, 1974). Briefly, the POI (2 mg/mL) was reacted with 0.2 M potassium cyanate (KOCN) in H_2O in a 1:1 v/v ratio for 24 h at 37°C. Typical reaction volumes were 0.5-1.0 mL. The reaction progress was analyzed by LC-MS (Waters UPLC). Upon completion of the reaction, carbamylated proteins were purified by gel filtration over Sephadex G-25 (PD-10 prepacked column, GE Healthcare). Purified proteins were stored at -80°C until further use.

In vitro Citrullination of Recombinant Proteins

Recombinant Vin and OVA variants were citrullinated as follows; 1 mg/mL of POI was dissolved in Tris-HCl (100 mM, pH=7.6) buffer containing $CaCl_2$ in ddH_2O (10 mM) and DTT (5 mM). Recombinant PAD4 (Sigma Aldrich, final concentration 1U) was added to the reaction mixture. Samples were incubated at 37°C for 5 h-o.n. under constant shaking (400 rpm). Upon completion of the reaction, citrullinated protein samples were purified via gel filtration and stored at -80°C for further use.

DEGRADATION ASSAYS

Bioorthogonal protein degradation *in cellulo*

Differentiated BMDCs were seeded in a tissue culture treated 24-well microtiter plate at 0.2 x 10^6 cells/well in 100-200 µL medium/well and were left to attach for 1 h. The bioorthogonal antigens dissolved in IMDM complete medium were added at the indicated concentrations over 1 h (pulse) at 37°C, 5% CO_2 under humidified air. Then the medium was aspirated gently, and the cells washed with pre-warmed IMDM medium. Subsequently, cells were pulsed for the indicated times (0-48h). The supernatant was then aspirated, and the cells resuspended in 50-100 µL of lysis buffer (100 mM Tris pH 7.5, 50 or 150 mM NaCl, complete protease inhibitor cocktail (EDTA-free), 0.25 % or 0.5 % CHAPS, 250 U Benzonase (Sigma, ref# E1014-25KU)) and incubated for 30 mins. The resulting samples were normalized by total protein concentration. For this purpose, the lysate was cleared via centrifugation (20000 g, 1h) and subjected either to Bradford assay (Biorad, the Netherlands, ref# 5000001) or Qubit Protein Assay (Thermo Fisher, the Netherlands, ref# Q33211)

20 µL of the normalized lysate was then mixed with 20 µL CuAAC-buffer. This buffer was generated via addition of following chemicals in the particular order: $CuSO_4$ in Milli-Q water (100 mM stock concentration, 6.4 mM final concentration), sodium ascorbate in Milli-Q water (1M stock concentration, 37.5 mM final concentration), followed by 2,4,6-Trimethoxybenzylidene-1,1,1-tris(hydroxymethyl) ethane methacrylate (TMTA) from a DMSO stock (100 mM, 10 µL, 1.3 mM final concentration) and Tris (stock concentration 100 mM, final concentration 88mM, pH 8.0). Finally, fluorophore-alkyne or –azides were added from DMSO-stocks (stock concentration 2 mM, 1-2 µL, 2.5-5 µM final concentration). Please note, upon addition of sodium ascorbate to $CuSO_4$, a color change from blue to brown (reduction of copper(II) into copper(I)) and finally to yellow should occur. Samples were incubated for 30 minutes at r.t. under gentile agitation (100-200 rpm) in the dark prior to the addition of Laemmli-buffer and SDS-PAGE analysis after which in-gel fluorescence was measured at the respective wavelengths and the specific protein amount was visualized by Coomassie staining.

T-CELL PROLIFERATION ASSAYS

***In vitro* MHC II-restricted Antigen Presentation Assay**

BMDCs were seeded (50,000/well, medium described above) in treated cell culture 96-well plates (flat bottom) and left at 37°C for 2h to allow adhesion. Then, cells were incubated with different concentrations of wild type and bioorthogonal versions, ranging from 0.4 to 93.3 µg/mL, for 6 h. Stock solutions of proteins were prepared in 10 mM $NaHCO_3$ and DMEM complete medium. The class II epitope of OVA (T_h epitope ISQAVHAAHAEINEAGR), was used as a positive control for antigen presentation. After the period of incubation, cells were washed with warm IMDM and $CD4^+$ OTII cells were added (50,000 cells/well, RPMI medium supplemented with 10% heat inactivated FCS, 2 mM glutamax, 50 µg/ml penicillin/streptomycin, 20 µM of β-mercaptoethanol). As a read out for T-cell activation, IL-2 secretion (ELISA) was measured in the supernatants 20 h later. Assays were performed in duplicates.

Human T-cell activation assay (Dendritic cell and Jurkat T-cell co-culture and evaluation of Jurkat activation)

Harvested dendritic cells were transferred to 96-wells plate, 3 wells per condition, except for the Jurkat only conditions. When the HLA-DQ/TCR interaction was blocked with antibodies, the dendritic cells were pre-incubated for 1 hour with 20 µg/mL anti-HLA-DQ (SPVL3) and anti-HLA-DR (B8.11.2) antibodies before Jurkat T-cells were added. JurkaT-cells were added to the wells in a 1:1 or a 1:2 ratio, keeping the number of Jurkat T-cells even. The cells were cultured together for ~16-18 hours before the cells were harvested, stained with Zombie NIR Fixable viability dye (Cat#: 423105, BioLegend) according to manufacturer's protocol and fixed with 3% paraformaldehyde. Cells were measured using the BD LSRFortessa. Results were analyzed using FlowJo Version 10.4.2.

ANALYTICAL METHODS

SDS-PAGE analysis (Laemmli, 1970)

For SDS-PAGE analysis all samples were heated for 5 minutes at 95°C except if they contained click cocktail heating was omitted. 20 µL of each sample was loaded onto a 15% SDS-PAGE gel and run for ~70 min at constant 170 V. Subsequently in-gel fluorescence was measured at the appropriate wavelengths after which a Coomassie staining (De St. Groth et al., 1963) or silver staining was performed using the SilverQuestion Staining protocol (Thermo Fisher Scientific, ref# LC6070) (Merril, 1990).

Circular Dichroism (CD)

All recombinant wt and bioorthogonal Vin and OVA variants were characterized via CD spectroscopy (Greenfield, 2006). Far UV-CD spectra were recorded using a Jasco J815 CD spectrometer equipped with a Jasco PTC 123 Peltier temperature controller (Easton, MD) between 190-260 nm. A minimum of five spectra with an acquisition time of 70 seconds (s) for each scan in a 1 mm quartz cuvette at 1 nm resolution were acquired at r.t. and averaged. Typical protein concentrations were between 0.1-0.3 mg/mL.

References

Ali, A.M.M.T., and S. Vino. 2016. Genetic markers as therapeutic target in rheumatoid arthritis: A game changer in clinical therapy? *Rheumatol. Int.* 36:1601-1607.

Angew Chem Int Ed EnglProceedings of the National Academy of SciencesMartínez, D., M. Vermeulen, E. von Euw, J. Sabatté, J. Maggíni, A. Ceballos, A. Trevani, K. Nahmod, G. Salamone, M. Barrio, M. Giordano, S. Amigorena, and J. Geffner. 2007. Extracellular Acidosis Triggers the Maturation of Human Dendritic Cells and the Production of IL-12. *J. Immunol.* 179:1950-1959.

Baka, Z., B. Gyorgy, P. Geher, E.I. Buzas, A. Falus, and G. Nagy. 2012. Citrullination under physiological and pathological conditions. *Joint Bone Spine* 79:431-436.

Bakkum, T., T. van Leeuwen, A.J.C. Sarris, D.M. van Elsland, D. Poulcharidis, H.S. Overkleeft, and S.I. van Kasteren. 2018. Quantification of Bioorthogonal Stability in Immune Phagocytes Using Flow Cytometry Reveals Rapid Degradation of Strained Alkynes. *ACS Chem. Biol.* 13:1173-1179.

Bang, H., K. Egerer, A. Gauliard, K. Lüthke, P.E. Rudolph, G. Fredenhagen, W. Berg, E. Feist, and G.-R. Burmester. 2007. Mutation and citrullination modifies vimentin to a novel autoantigen for rheumatoid arthritis. *Arthritis Rheum.* 56:2503-2511.

Barnden, M.J., J. Allison, W.R. Heath, and F.R. Carbone. 1998a. Defective TCR expression in transgenic mice constructed using cDNA-based α- and β-chain genes under the control of heterologous regulatory elements. *Immunol. Cell Biol.* 76:34.

Barnden, M.J., J. Allison, W.R. Heath, and F.R. Carbone. 1998b. Defective TCR expression in transgenic mice constructed using cDNA-based α- and β-chain genes under the control of heterologous regulatory elements. *Immunol. Cell Biol.* 76:34-40.

Blachère, N.E., S. Parveen, M.O. Frank, B.D. Dill, H. Molina, and D.E. Orange. 2017. High-Titer Rheumatoid Arthritis Antibodies Preferentially Bind Fibrinogen Citrullinated by Peptidylarginine Deiminase 4. *Arthritis Rheumatol.* 69:986-995.

Buck, S.B., J. Bradford, K.R. Gee, B.J. Agnew, S.T. Clarke, and A. Salic. 2008. Detection of S-phase cell cycle progression using 5-ethynyl-2 '-deoxyuridine incorporation with click chemistry an alternative to using 5-bromo-2 '-deoxyuridine antibodies. *BioTechniques* 44:927-929.

Burgdorf, S., A. Kautz, V. Bohnert, P.A. Knolle, and C. Kurts. 2007. Distinct pathways of antigen uptake and intracellular routing in CD4 and CD8 T cell activation. *Science* 316:612-616.

Burgdorf, S., V. Schuette, V. Semmling, K. Hochheiser, V. Lukacs-Kornek, P.A. Knolle, and C. Kurts. 2010. Steady-state cross-presentation of OVA is mannose receptor-dependent but inhibitable by collagen fragments. *Proc. Natl. Acad. Sci.* 107:E48-E49.

Castellino, F., F. Zappacosta, J.E. Coligan, and R.N. Germain. 1998. Large Protein Fragments as Substrates for Endocytic Antigen Capture by MHC Class II Molecules. *J. Immunol.* 161:4048-4057.

Cebrian, I., G. Visentin, N. Blanchard, M. Jouve, A. Bobard, C. Moita, J. Enninga, L.F. Moita, S. Amigorena, and A. Savina. 2011. Sec22b Regulates Phagosomal Maturation and Antigen Crosspresentation by Dendritic Cells. *Cell* 147:1355-1368.

Chang, C.T., C.S. Wu, and J.T. Yang. 1978. Circular dichroic analysis of protein conformation: inclusion of the beta-turns. *Anal. Biochem.* 91:13-31.

Chang, X., R. Yamada, A. Suzuki, Y. Kochi, T. Sawada, and K. Yamamoto. 2005. Citrullination of fibronectin in rheumatoid arthritis synovial tissue. *Rheumatology (Oxford)* 44:1374-1382.

De St. Groth, S.F., R.G. Webster, and A. Datyner. 1963. Two new staining procedures for quantitative estimation of proteins on electrophoretic strips. *Biochim. Biophys. Acta* 71:377-391.

Del Cid, N., L. Shen, J. BelleIsle, and M. Raghavan. 2012. Assessment of Roles for Calreticulin in the Cross-Presentation of Soluble and Bead-Associated Antigens. *PLOS ONE* 7:e41727.

Fando, J., and S. Grisolia. 1974. Carbamylation of brain proteins with cyanate in vitro and in vivo. *Eur. J. Biochem.* 47:389-396.

Fazilleau, N., L. Mark, L.J. McHeyzer-Williams, and M.G. McHeyzer-Williams. 2009. Follicular Helper T Cells: Lineage and Location. *Immunity* 30:324-335.

Fearon, W.R. 1939. The carbamido diacetyl reaction: a test for citrulline. *Biochem J* 33:902-907.

Firestein, G.S., and I.B. McInnes. 2017. Immunopathogenesis of Rheumatoid Arthritis. *Immunity* 46:183-196.

Giodini, A., and P. Cresswell. 2008. Hsp90-mediated cytosolic refolding of exogenous proteins internalized by dendritic cells. *Embo J.* 27:201-211.

Greenfield, N.J. 2006. Using circular dichroism spectra to estimate protein secondary structure. *Nat. Protoc.* 1:2876-2890.

Guan, K.L., W. Yu, Y. Lin, Y. Xiong, and S. Zhao. 2010. Generation of acetyllysine antibodies and affinity enrichment of acetylated peptides. *Nat. Protoc.* 5:1583-1595.

György, B., E. Tóth, E. Tarcsa, A. Falus, and E.I. Buzás. 2006. Citrullination: A posttranslational modification in health and disease. *Int. J. Biochem. Cell Biol.* 38:1662-1677.

Hang, H.C., J.P. Wilson, and G. Charron. 2011. Bioorthogonal chemical reporters for analyzing protein lipidation and lipid trafficking. *Acc. Chem. Res.* 44:699-708.

Hill, J.A., S. Southwood, A. Sette, A.M. Jevnikar, D.A. Bell, and E. Cairns. 2003. Cutting Edge: The Conversion of Arginine to Citrulline Allows for a High-Affinity Peptide Interaction with the Rheumatoid Arthritis-Associated HLA-DRB1*0401 MHC Class II Molecule. *J. Immunol.* 171:538-541.

Ho, N.I., M.G.M. Camps, E.F.E. de Haas, L.A. Trouw, J.S. Verbeek, and F. Ossendorp. 2017. C1q-Dependent Dendritic Cell Cross-Presentation of In Vivo–Formed Antigen–Antibody Complexes. *J. Immunol.* 198:4235-4243.

Hoogendoorn, S., G.H.M. van Puijvelde, J. Kuiper, G.A. van der Marel, and H.S. Overkleeft. 2014. A Multivalent Ligand for the Mannose-6-Phosphate Receptor for Endolysosomal Targeting of an Activity-Based Probe. *Angew. Chem. Int. Ed. Engl.* 53:10975-10978.

Huse, M., L.O. Klein, A.T. Girvin, J.M. Faraj, Q.J. Li, M.S. Kuhns, and M.M. Davis. 2007. Spatial and temporal dynamics of T cell receptor signaling with a photoactivatable agonist. *Immunity* 27:76-88.

Inaba, K., M. Inaba, N. Romani, H. Aya, M. Deguchi, S. Ikehara, S. Muramatsu, and R.M. Steinman. 1992. Generation of large numbers of dendritic cells from mouse bone marrow cultures supplemented with granulocyte/macrophage colony-stimulating factor. *J. Exp. Med.* 176:1693-1702.

Chang, P.V., J.A. Prescher, E.M. Sletten, J.M. Baskin, I.A. Miller, N.J. Agard, A. Lo, and C.R. Bertozzi. 2010. Copper-free click chemistry in living animals. *Proc. Natl. Acad. Sci.* 107: 1821–1826.

Jiang, X., L.A. Trouw, T.J. van Wesemael, J. Shi, C. Bengtsson, H. Källberg, V. Malmström, L. Israelsson, H. Hreggvidsdottir, W. Verduijn, L. Klareskog, L. Alfredsson, T.W.J. Huizinga, R.E.M. Toes, K. Lundberg, and D. van der Woude. 2014. Anti-CarP antibodies in two large cohorts of patients with

rheumatoid arthritis and their relationship to genetic risk factors, cigarette smoking and other autoantibodies. *Ann. Rheum. Dis.* 73:1761-1768.

Jones, J.D., B.J. Hamilton, and W.F.C. Rigby. 2017. Brief Report: Anti–Carbamylated Protein Antibodies in Rheumatoid Arthritis Patients Are Reactive With Specific Epitopes of the Human Fibrinogen β-Chain. *Arthritis Rheumatol.* 69:1381-1386.

Jutz, S., J. Leitner, K. Schmetterer, I. Doel-Perez, O. Majdic, K. Grabmeier-Pfistershammer, W. Paster, J.B. Huppa, and P. Steinberger. 2016. Assessment of costimulation and coinhibition in a triple parameter T cell reporter line: Simultaneous measurement of NF-κB, NFAT and AP-1. *J. Immunol. Methods* 430:10-20.

Kampstra, A.S.B., and R.E.M. Toes. 2017. HLA class II and rheumatoid arthritis: the bumpy road of revelation. *Immunogenetics* 69: 597-603.

Kiick, K.L., E. Saxon, D.A. Tirrell, and C.R. Bertozzi. 2002. Incorporation of azides into recombinant proteins for chemoselective modification by the Staudinger ligation. *Proc. Natl. Acad. Sci. U S A* 99:19-24.

Kiick, K.L., and D.A. Tirrell. 2000. Protein engineering by in vivo incorporation of non-natural amino acids: Control of incorporation of methionine analogues by methionyl-tRNA synthetase. *Tetrahedron* 56:9487-9493.

Kiick, K.L., R. Weberskirch, and D.A. Tirrell. 2001. Identification of an expanded set of translationally active methionine analogues in Escherichia coli. *FEBS Lett.* 502:25-30.

Kokkonen, H., M. Mullazehi, E. Berglin, G. Hallmans, G. Wadell, J. Ronnelid, and S. Rantapaa-Dahlqvist. 2011. Antibodies of IgG, IgA and IgM isotypes against cyclic citrullinated peptide precede the development of rheumatoid arthritis. *Arthritis Res Ther* 13:R13.

Laconte, L., N. Nitin, and G. Bao. 2005. Magnetic nanoparticle probes. *Mater. Today (Kidlington)* 8:32-38.

Laemmli, U.K. 1970. Cleavage of Structural Proteins during the Assembly of the Head of Bacteriophage T4. *Nature* 227:680.

Lang, K., and J.W. Chin. 2014. Bioorthogonal reactions for labeling proteins. *ACS Chem. Biol.* 9:16-20.

Leahy, D.J., W.A. Hendrickson, I. Aukhil, and H.P. Erickson. 1992. Structure of a fibronectin type III domain from tenascin phased by MAD analysis of the selenomethionyl protein. *Science* 258:987-991.

Lutz, M.B., N. Kukutsch, A.L.J. Ogilvie, S. Rößner, F. Koch, N. Romani, and G. Schuler. 1999. An advanced culture method for generating large quantities of highly pure dendritic cells from mouse bone marrow. *J. Immunol. Methods* 223:77-92.

MacGregor, A., W. Ollier, W. Thomson, D. Jawaheer, and A. Silman. 1995. HLA-DRB1*0401/0404 genotype and rheumatoid arthritis: increased association in men, young age at onset, and disease severity. *J. Rheumatol.* 22:1032-1036.

Manganelli, V., S. Recalchi, A. Capozzi, G. Riitano, V. Mattei, A. Longo, M. Di Franco, C. Alessandri, M. Bombardieri, G. Valesini, R. Misasi, T. Garofalo, and M. Sorice. 2018. Autophagy induces protein carbamylation in fibroblast-like synoviocytes from patients with rheumatoid arthritis. *Rheumatology (Oxford)*

Merril, C.R. 1990. [36] Gel-staining techniques. In Methods in Enzymology. M.P. Deutscher, editor Academic Press, 477-488.

Moss, C.X., T.I. Tree, and C. Watts. 2007. Reconstruction of a pathway of antigen processing and class II MHC peptide capture. *Embo J.* 26:2137-2147.

Moudgil, K.D., and E.E. Sercarz. 1994. The T Cell Repertoire against Cryptic Self Determinants and Its Involvement in Autoimmunity and Cancer. *Clin. Immunol. Immunopathol.* 73:283-289.

Mydel, P., Z. Wang, M. Brisslert, A. Hellvard, L.E. Dahlberg, S.L. Hazen, and M. Bokarewa. 2010. Carbamylation-dependent activation of T cells: a novel mechanism in the pathogenesis of autoimmune arthritis. *J. Immunol.* 184:6882-6890.

Norbury, C.C., B.J. Chambers, A.R. Prescott, H.G. Ljunggren, and C. Watts. 1997. Constitutive macropinocytosis allows TAP-dependent major histocompatibility complex class I presentation of exogenous soluble antigen by bone marrow-derived dendritic cells. *Eur J Immunol* 27:280-288.

Pawlak, J.B., G.P. Gential, T.J. Ruckwardt, J.S. Bremmers, N.J. Meeuwenoord, F.A. Ossendorp, H.S. Overkleeft, D.V. Filippov, and S.I. van Kasteren. 2015. Bioorthogonal Deprotection on the Dendritic Cell Surface for Chemical Control of Antigen Cross-Presentation. *Angew. Chem. Int. Ed. Engl.* 54:5628-5631.

Pickering, A.M., and K.J.A. Davies. 2012. A simple fluorescence labeling method for studies of protein oxidation, protein modification, and proteolysis. *Free Radic. Biol. Med.* 52:239-246.

Princiotta, M.F., D. Finzi, S.-B. Qian, J. Gibbs, S. Schuchmann, F. Buttgereit, J.R. Bennink, and J.W. Yewdell. 2003. Quantitating Protein Synthesis, Degradation, and Endogenous Antigen Processing. *Immunity* 18:343-354.

Pruijn, G.J. 2015. Citrullination and carbamylation in the pathophysiology of rheumatoid arthritis. *Front. Immunol.* 6:192.

Qin, L.-H., W. Hu, and Y.-Q. Long. 2018. Bioorthogonal Chemistry: Optimization and Application Updates during 2013-2017. *Tetrahedron Lett.*

Ramil, C.P., and Q. Lin. 2013. Bioorthogonal chemistry: strategies and recent developments. *Chem. Commun.* 49:11007-11022.

Rantapää-Dahlqvist, S., B.A.W. de Jong, E. Berglin, G. Hallmans, G. Wadell, H. Stenlund, U. Sundin, and W.J. van Venrooij. 2003. Antibodies against cyclic citrullinated peptide and IgA rheumatoid factor predict the development of rheumatoid arthritis. *Arthritis Rheum.* 48:2741-2749.

Rosskopf, S., J. Leitner, W. Paster, L.T. Morton, R.S. Hagedoorn, P. Steinberger, and M.H.M. Heemskerk. 2018. A Jurkat 76 based triple parameter reporter system to evaluate TCR functions and adoptive T cell strategies. *Oncotarget* 9:17608-17619.

Rostovtsev, V.V., L.G. Green, V.V. Fokin, and K.B. Sharpless. 2002. A stepwise huisgen cycloaddition process: copper(I)-catalyzed regioselective "ligation" of azides and terminal alkynes. *Angew. Chem. Int. Ed. Engl.* 41:2596-2599.

Saxon, E., and C.R. Bertozzi. 2000. Cell surface engineering by a modified Staudinger reaction. *Science* 287:2007-2010.

Scally, S.W., J. Petersen, S.C. Law, N.L. Dudek, H.J. Nel, K.L. Loh, L.C. Wijeyewickrema, S.B. Eckle, J. van Heemst, R.N. Pike, J. McCluskey, R.E. Toes, N.L. La Gruta, A.W. Purcell, H.H. Reid, R. Thomas, and J. Rossjohn. 2013. A molecular basis for the association of the HLA-DRB1 locus, citrullination, and rheumatoid arthritis. *J. Exp. Med.* 210:2569-2582.

Scherer, H.U., T.W.J. Huizinga, G. Kronke, G. Schett, and R.E.M. Toes. 2018. The B cell response to citrullinated antigens in the development of rheumatoid arthritis. *Nat. Rev. Rheumatol.* 14:157-169.

Schwenzer, A., X. Jiang, T.R. Mikuls, J.B. Payne, H.R. Sayles, A.M. Quirke, B.M. Kessler, R. Fischer, P.J. Venables, K. Lundberg, and K.S. Midwood. 2016. Identification of an immunodominant peptide from citrullinated tenascin-C as a major target for autoantibodies in rheumatoid arthritis. *Ann. Rheum. Dis.* 75:1876-1883.

Sercarz, E.E., P.V. Lehmann, A. Ametani, G. Benichou, A. Miller, and K. Moudgil. 1993. Dominance and crypticity of T-cell antigenic determinants. *Ann. Rheum. Dis.* 11:729-766.

Shen, L., L.J. Sigal, M. Boes, and K.L. Rock. 2004. Important Role of Cathepsin S in Generating Peptides for TAP-Independent MHC Class I Crosspresentation In Vivo. *Immunity* 21:155-165.

Shi, J., R. Knevel, P. Suwannalai, M.P. van der Linden, G.M.C. Janssen, P.A. van Veelen, N.E.W. Levarht, A.H.M. van der Helm-van Mil, A. Cerami, T.W.J. Huizinga, R.E.M. Toes, and L.A. Trouw. 2011. Autoantibodies recognizing carbamylated proteins are present in sera of patients with rheumatoid arthritis and predict joint damage. *Proc. Natl. Acad. Sci.* 108:17372-17377.

Siegrist, M.S., S. Whiteside, J.C. Jewett, A. Aditham, F. Cava, and C.R. Bertozzi. 2012. d-Amino Acid Chemical Reporters Reveal Peptidoglycan Dynamics of an Intracellular Pathogen. *ACS Chem. Biol.* 8:500-505.

Sletten, E.M., and C.R. Bertozzi. 2009. Bioorthogonal chemistry: fishing for selectivity in a sea of functionality. *Angew. Chem. Int. Ed. Engl.* 48:6974-6998.

Snijders, A., D.G. Elferink, A. Geluk, A.L. van der Zanden, K. Vos, G.M.T. Schreuder, F.C. Breedveld, R.R.P. de Vries, and E.H. Zanelli. 2001. An HLA-DRB1-Derived Peptide Associated with Protection Against Rheumatoid Arthritis Is Naturally Processed by Human APCs. *J. Immunol.* 166:4987-4993.

Stark, G.R., W.H. Stein, and S. Moore. 1960. Reactions of the Cyanate Present in Aqueous Urea with Amino Acids and Proteins. *J. Biol. Chem.* 235:3177-3181.

Stern, L.J., J.H. Brown, T.S. Jardetzky, J.C. Gorga, R.G. Urban, J.L. Strominger, and D.C. Wiley. 1994. Crystal structure of the human class II MHC protein HLA-DR1 complexed with an influenza virus peptide. *Nature* 368:215.

T., Z., M. Y., H. J., D. T., N.B. F., H. H., S. T, A. T, H. K., G.R. A., and K. N. 2000. Lysosomal cathepsin B plays an important role in antigen processing, while cathepsin D is involved in degradation of the invariant chain in ovalbumin-immunized mice. *Immunology* 100:13-20.

Tarcsa, E., L.N. Marekov, G. Mei, G. Melino, S.C. Lee, and P.M. Steinert. 1996. Protein unfolding by peptidylarginine deiminase. Substrate specificity and structural relationships of the natural substrates trichohyalin and filaggrin. *J. Biol. Chem.* 271:30709-30716.

Titcombe, P.J., G. Wigerblad, N. Sippl, N. Zhang, A.K. Shmagel, P. Sahlstrom, Y. Zhang, L.O. Barsness, Y. Ghodke-Puranik, A. Baharpoor, M. Hansson, L. Israelsson, K. Skriner, T.B. Niewold, L. Klareskog, C.I. Svensson, K. Amara, V. Malmstrom, and D.L. Mueller. 2018. Pathogenic citrulline-multispecific B cell receptor clades in rheumatoid arthritis. *Arthritis Rheum.*

Tornøe, C.W., C. Christensen, and M. Meldal. 2002. Peptidotriazoles on Solid Phase: [1,2,3]-Triazoles by Regiospecific Copper(I)-Catalyzed 1,3-Dipolar Cycloadditions of Terminal Alkynes to Azides. *J. Org. Chem.* 67:3057-3064.

Travers, T.S., L. Harlow, I.O. Rosas, B.R. Gochuico, T.R. Mikuls, S.K. Bhattacharya, C.J. Camacho, and D.P. Ascherman. 2016. Extensive Citrullination Promotes Immunogenicity of HSP90 through Protein Unfolding and Exposure of Cryptic Epitopes. *J. Immunol*. 197:1926-1936.

Trombetta, E.S., M. Ebersold, W. Garrett, M. Pypaert, and I. Mellman. 2003. Activation of Lysosomal Function During Dendritic Cell Maturation. *Science* 299:1400-1403.

Trouw, L.A., T. Rispens, and R.E.M. Toes. 2017. Beyond citrullination: other post-translational protein modifications in rheumatoid arthritis. *Nat. Rev. Rheumatol.* 13:331-339.

Truchetet, M.E., S. Dublanc, T. Barnetche, O. Vittecoq, X. Mariette, C. Richez, P. Blanco, M. Mahler, C. Contin-Bordes, T. Schaeverbeke, and A. Federation Hospitalo-Universitaire. 2017. Association of the Presence of Anti-Carbamylated Protein Antibodies in Early Arthritis With a Poorer Clinical and Radiologic Outcome: Data From the French ESPOIR Cohort. *Arthritis Rheum.* 69:2292-2302.

Unanue, E.R., V. Turk, and J. Neefjes. 2016. Variations in MHC Class II Antigen Processing and Presentation in Health and Disease. *Ann. Rheum. Dis.* 34:265-297.

van Beers, J.J., C.M. Schwarte, J. Stammen-Vogelzangs, E. Oosterink, B. Bozic, and G.J. Pruijn. 2013. The rheumatoid arthritis synovial fluid citrullinome reveals novel citrullinated epitopes in apolipoprotein E, myeloid nuclear differentiation antigen, and beta-actin. *Arthritis Rheum.* 65:69-80.

van Dalen, C.J., M.W. Whitehouse, C.C. Winterbourn, and A.J. Kettle. 1997. Thiocyanate and chloride as competing substrates for myeloperoxidase. *Biochem J*. 327 (Pt 2):487-492.

van der Gracht, A.M.F., M.A.R. de Geus, M.G.M. Camps, T.J. Ruckwardt, A.J.C. Sarris, J. Bremmers, E. Maurits, J.B. Pawlak, M.M. Posthoorn, K.M. Bonger, D.V. Filippov, H.S. Overkleeft, M.S. Robillard, F. Ossendorp, and S.I. van Kasteren. 2018. Chemical Control over T-Cell Activation in Vivo Using Deprotection of trans-Cyclooctene-Modified Epitopes. *ACS Chem. Biol.* 13: 1569–1576.

van der Woude, D., and A.I. Catrina. 2015. HLA and anti-citrullinated protein antibodies: Building blocks in RA. *Best Pract. Res. Clin. Rheumatol*. 29:692-705.

van Elsland, D.M., E. Bos, W. de Boer, H.S. Overkleeft, A.J. Koster, and S.I. van Kasteren. 2016. Detection of bioorthogonal groups by correlative light and electron microscopy allows imaging of degraded bacteria in phagocytes. *Chem. Sci*. 7:752-758.

van Geel, R., G.J.M. Pruijn, F.L. van Delft, and W.C. Boelens. 2012. Preventing Thiol-Yne Addition Improves the Specificity of Strain-Promoted Azide-Alkyne Cycloaddition. *Bioconj. Chem.* 23:392-398.

van Heemst, J., D.T. Jansen, S. Polydorides, A.K. Moustakas, M. Bax, A.L. Feitsma, D.G. Bontrop-Elferink, M. Baarse, D. van der Woude, G.J. Wolbink, T. Rispens, F. Koning, R.R. de Vries, G.K. Papadopoulos, G. Archontis, T.W. Huizinga, and R.E. Toes. 2015. Crossreactivity to vinculin and microbes provides a molecular basis for HLA-based protection against rheumatoid arthritis. *Nat. Commun*. 6:6681.

van Hest, J.C.M., K.L. Kiick, and D.A. Tirrell. 2000. Efficient Incorporation of Unsaturated Methionine Analogues into Proteins in Vivo. *J. Am. Chem. Soc*. 122:1282-1288.

van Kasteren, S.I., H.B. Kramer, D.P. Gamblin, and B.G. Davis. 2007a. Site-selective glycosylation of proteins: creating synthetic glycoproteins. *Nat. Protoc.* 2:3185-3194.

van Kasteren, S.I., H.B. Kramer, H.H. Jensen, S.J. Campbell, J. Kirkpatrick, N.J. Oldham, D.C. Anthony, and B.G. Davis. 2007b. Expanding the diversity of chemical protein modification allows post-translational mimicry. *Nature* 446:1105-1109.

van Kasteren, S.I., and H.S. Overkleeft. 2014. Endo-lysosomal proteases in antigen presentation. *Curr. Opin. Chem. Biol*. 23:8-15.

van Montfoort, N., M.G. Camps, S. Khan, D.V. Filippov, J.J. Weterings, J.M. Griffith, H.J. Geuze, T. van Hall, J.S. Verbeek, C.J. Melief, and F. Ossendorp. 2009. Antigen storage compartments in mature dendritic cells facilitate prolonged cytotoxic T lymphocyte cross-priming capacity. *Proc. Natl. Acad. Sci*. 106:6730-6735.

van Venrooij, W.J., J.J. van Beers, and G.J. Pruijn. 2011. Anti-CCP antibodies: the past, the present and the future. *Nat. Rev. Rheumatol*. 7:391-398.

Vander Cruyssen, B., T. Cantaert, L. Nogueira, C. Clavel, L. De Rycke, A. Dendoven, M. Sebag, D. Deforce, C. Vincent, D. Elewaut, G. Serre, and F. De Keyser. 2006. Diagnostic value of anti-human citrullinated fibrinogen ELISA and comparison with four other anti-citrullinated protein assays. *Arthritis Res. Ther*. 8:R122-R122.

Voss, E.W., Jr., C.J. Workman, and M.E. Mummert. 1996. Detection of protease activity using a fluorescence-enhancement globular substrate. *BioTechniques* 20:286-291.

Vossenaar, E.R., A.J. Zendman, W.J. van Venrooij, and G.J. Pruijn. 2003. PAD, a growing family of citrullinating enzymes: genes, features and involvement in disease. *Bioessays* 25:1106-1118.

Walker, M.W., and E. Lloyd–Evans. 2015. Chapter 2 - A rapid method for the preparation of ultrapure, functional lysosomes using functionalized superparamagnetic iron oxide nanoparticles. In Methods in Cell Biology. F. Platt, and N. Platt, editors. Academic Press, 21-43.

Wals, K., and H. Ovaa. 2014. Unnatural amino acid incorporation in E. coli: current and future applications in the design of therapeutic proteins. *Front. Chem.* 2:15.

West, M.A., R.P.A. Wallin, S.P. Matthews, H.G. Svensson, R. Zaru, H.G. Ljunggren, A.R. Prescott, and C. Watts. 2004. Enhanced dendritic cell antigen capture via Toll-like receptor-induced actin remodeling. *Science* 305:1153-1157.

Wood, W.B. 1966. Host specificity of DNA produced by Escherichia coli: bacterial mutations affecting the restriction and modification of DNA. *J. Mol. Biol.* 16:118-133.

Zaidi, N., T. Herrmann, D. Baechle, S. Schleicher, J. Gogel, C. Driessen, W. Voelter, and H. Kalbacher. 2007. A new approach for distinguishing cathepsin E and D activity in antigen-processing organelles. *FEBS J.* 274:3138-3149.

Zhang, M.M., L.K. Tsou, G. Charron, A.S. Raghavan, and H.C. Hang. 2010. Tandem fluorescence imaging of dynamic S-acylation and protein turnover. *Proc. Natl. Acad. Sci.* 107:8627-8632.

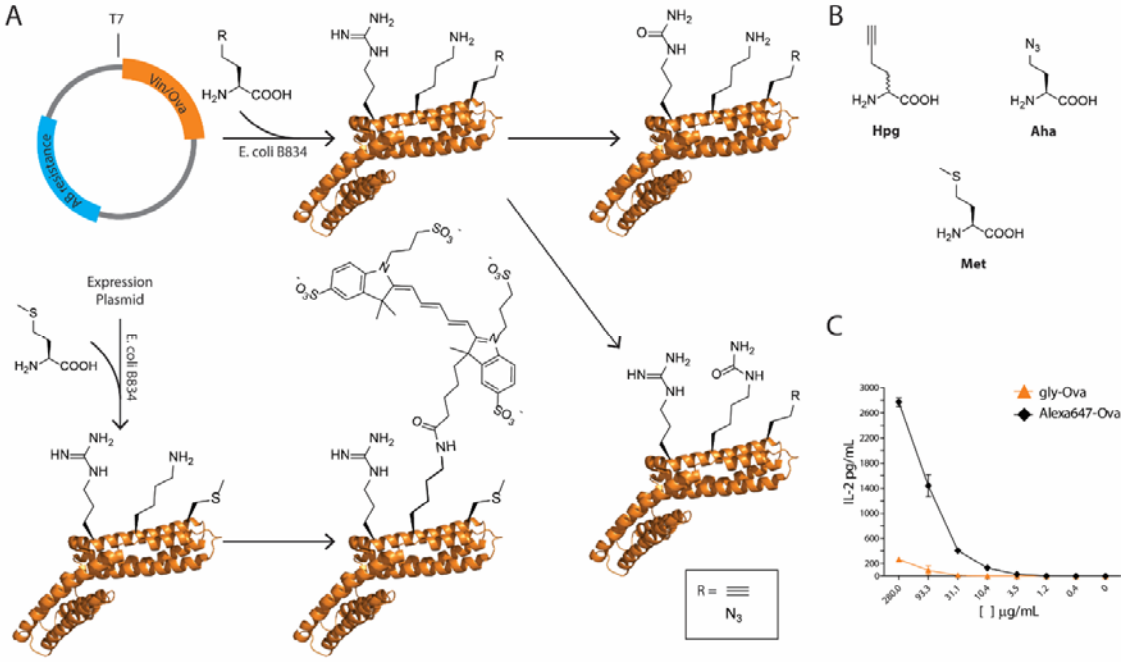

Figure 1**:** ***Production of citrullinated and carbamylated bioorthogonal antigens.*** A: protein of interest can be expressed with methionine and fluorophore modified (bottom arrow); alternatively, the protein can be expressed with bioorthogonal amino acids to replace methionine. These proteins can then be carbamylated chemically, or citrullinated using recombinant PAD enzymes (top arrows); B: structures of unnatural amino acids homopropargylglycine (**Hpg**) and azidohomoalanine (**Aha**) compared to methionine (**Met**); C: ELISA measurements of IL-2 [pg/mL] from mouse OT-II T-cells incubated with commercially available Ova isolated from chicken eggs (gly-OVA, orange triangles) and an Alexa-647-fluorophore labeled variant of the same protein (Alexa-647-OVA, black diamond).

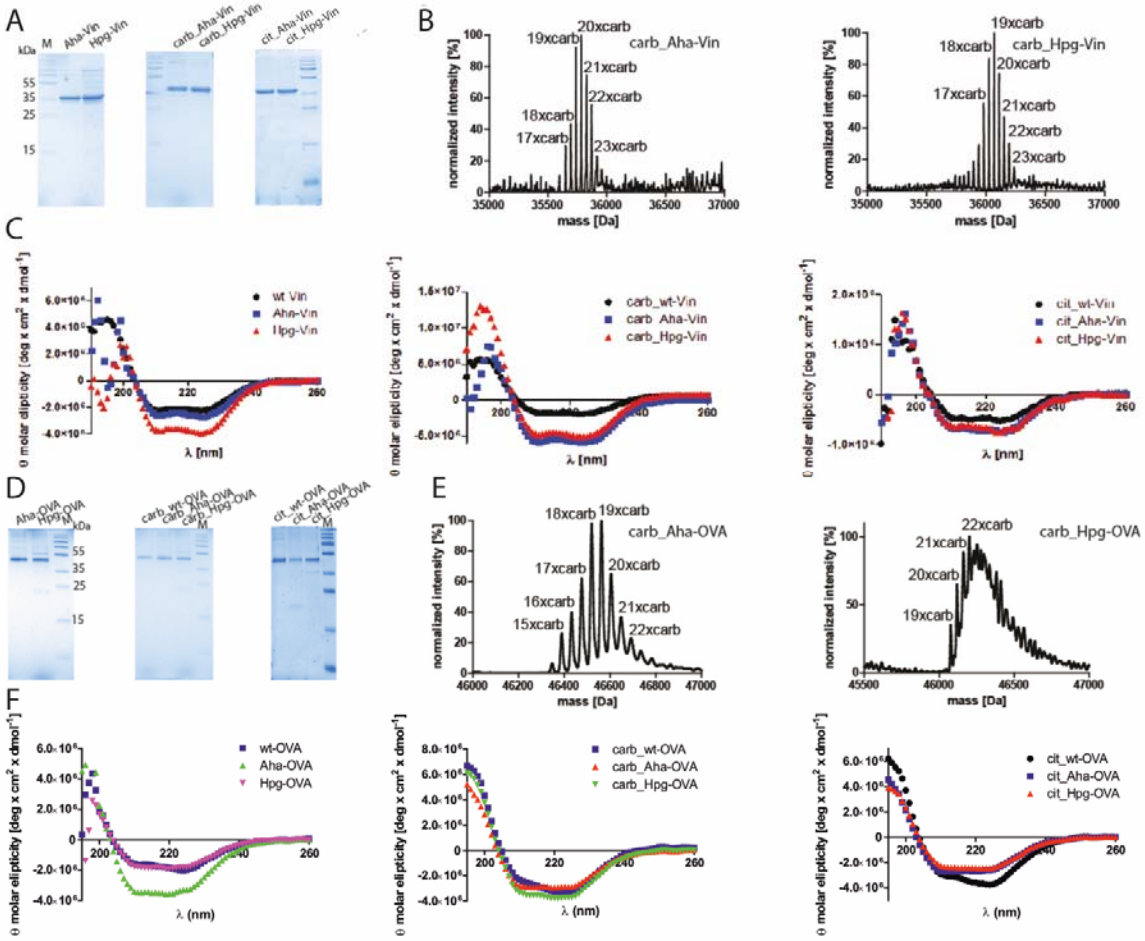

Figure 2: ***BONCAT expression and characterization of bioorthogonal Vin and Ova derivatives.*** A: SDS-PAGE analysis of purified, non-modified (left), carbamylated (middle) or citrullinated (right) bioorthogonal Vin derivatives. B**:** TOF-MS analysis of carbamylated bioorthogonal Vin derivatives**,** left; carb_Aha-Vin (mixed species from 17x-to 23x-carbamylated Aha-Vin, no traces of non-carbamylated Aha-Vin), right; carb_Hpg-Vin (mixed species from 17x-to 23x-carbamylated Hpg-Vin, no traces of non-carbamylated Hpg-Vin) C: Biophysical characterization of bioorthogonal antigens via circular dichroism (CD) spectroscopy, left panel: wt- (black circles), Aha- (blue squares) and Hpg-Vin (red triangles), middle panel: carbamylated Vin derivatives, right panel: citrullinated Vin derivatives. D: SDS-PAGE analysis of purified, non-modified (left), carbamylated (middle) or citrullinated (right) bioorthogonal Ova derivatives, E: TOF-MS analysis of carbamylated bioorthogonal Ova derivatives, left; carb_Aha-Ova (mixed species from 15x-to 22x-carbamylated Aha-Ova, no traces of non-carbamylated Aha-OVA), right; carb_Hpg-Ova (mixed species from 19x-to 22x-carbamylated Hpg-Ova, no traces of non-carbamylated Hpg-Ova), F: Biophysical characterization of bioorthogonal Ova variants via CD, left panel: wt- (blue squares), Aha- (green triangles) and Hpg-Vin (magenta triangles); middle panel: carbamylated Ova derivatives, right panel: citrullinated Ova derivatives.

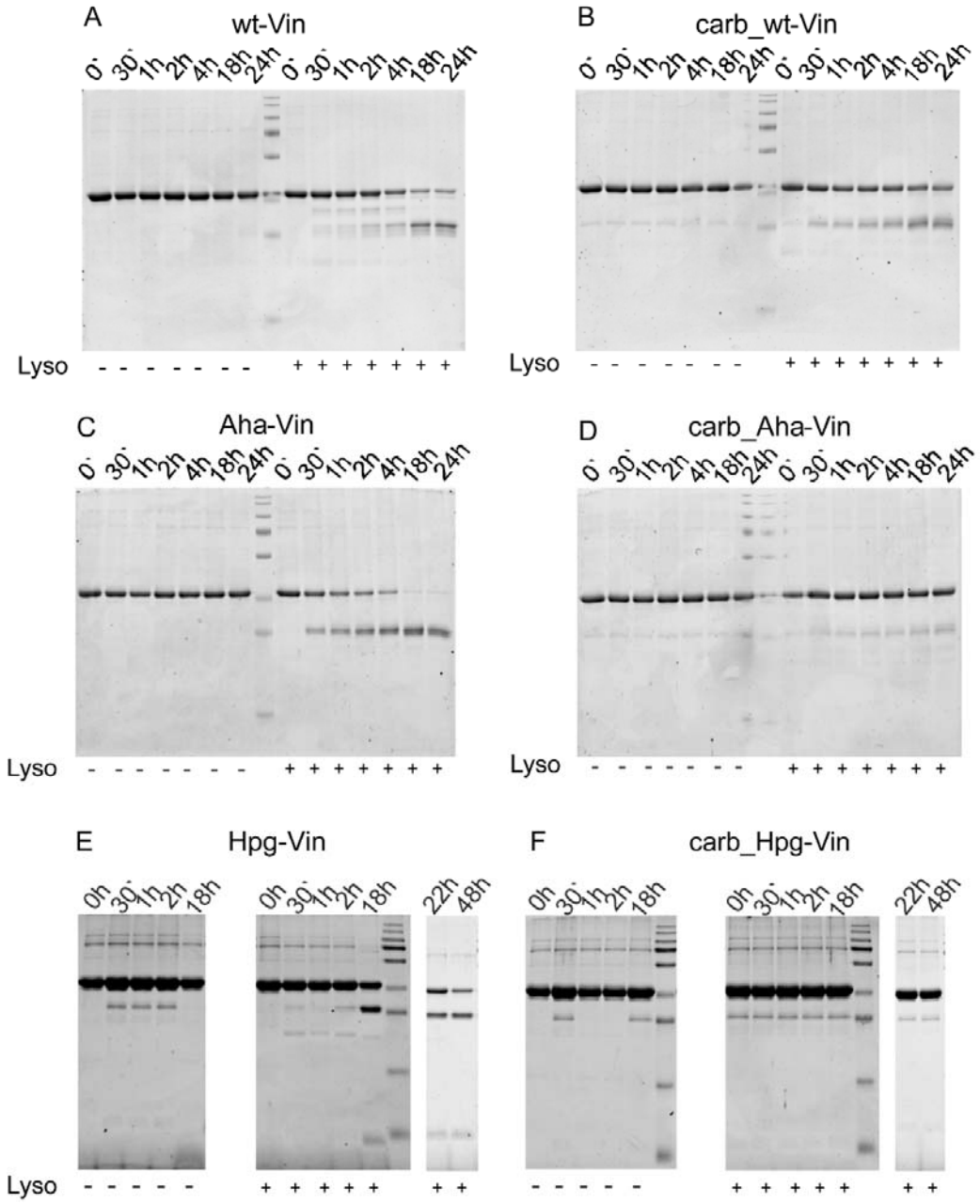

Figure 3: ***Proteolysis of bioorthogonal Vin in vitro.***
Wt and bioorthogonal Vin derivatives were treated with lysosomes (18 µg total amount of lysosomal proteins) at pH 5.0 and analyzed via SDS-PAGE (Coomassie Staining). A: wt-Vin incubated with lysosomes extracts (Lyso +) for 0h, 30min, 1h, 2h, 4h, 18h and 24h. B: carb_wt-Vin incubated with lysosomes extracts for 0h, 30 min, 1h, 2h, 4h, 18h and 24h. (Lyso -) : samples incubated with the lysosomal buffer in the absence of lysosomes (control samples), total amount of Vin per lane 2.5 µg. C: Aha-Vin incubated with lysosomes extracts (Lyso +) for 0h, 30 min, 1h, 2h, 4h, 18h and 24h. D: carb_Aha-Vin incubated with lysosomes extracts for 0h, 30 min, 1h, 2h, 4h, 18h and 24h. (Lyso -) : samples not incubated with lysosomes (control samples), total amount of Vin per lane 2.5 µg. E: Hpg-Vin incubated with lysosomes extracts for 0h, 30 min, 1h, 2h and 18h. Left**;** Hpg-Vin without lysosomes (control samples), right; Hpg-Vin incubated with lysosomes. F: carb_Hpg-Vin incubated with lysosomes extracts for 0h, 30 min, 1h, 2h and 18h. Left**;** carb_Hpg-Vin without lysosomes (control samples), right; carb_Hpg-Vin incubated with lysosomes. Total amount of Hpg-Vin per lane 5 µg. At least two independent experiments were conducted.

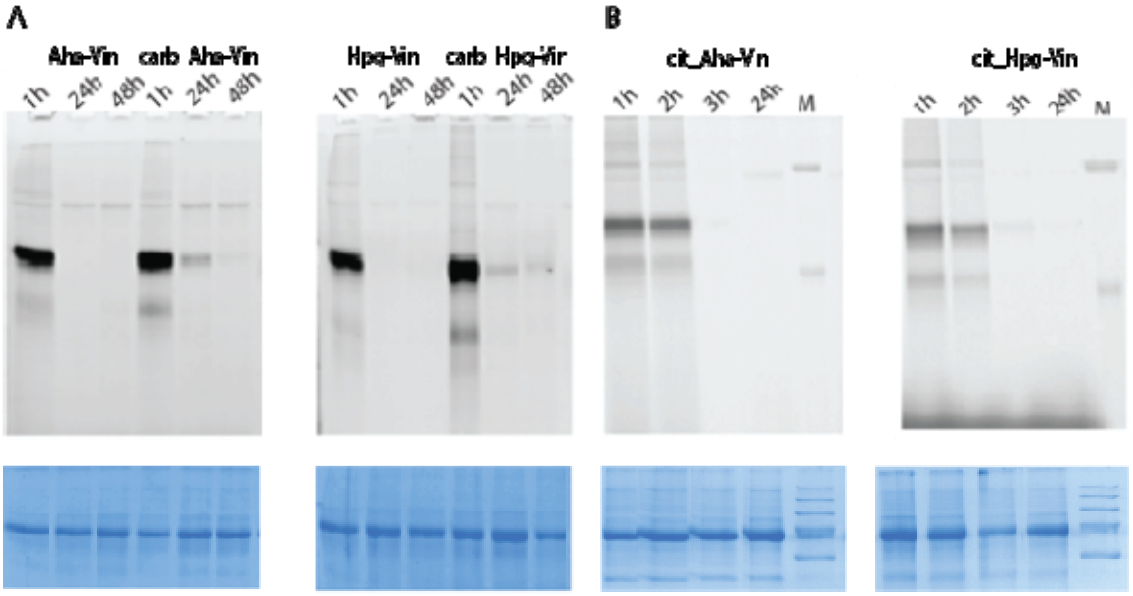

Figure 4: ***Analysis of antigen proteolysis in BMDCs*** Cells were pulsed with bioorthogonal antigens for two hours and chased for the indicated timepoints. After these the cells were collected, lysed and subjected to CuAAC conditions to introduce AlexaFluor-488 with alkyne or azide functionality followed by the separation of proteinogenic cell lysate components via SDS-PAGE analysis. A: degradation of bioorthogonal type and carbamylated Vin (grey: fluorescent signal from AlexaFluor-488; blue: Coomassie loading control); B: Degradation of citrullinated, bioorthogonal Vinculin (left, citrullinated Aha-Vin, right citrullinated Hpg-Vin); M: protein ladder.

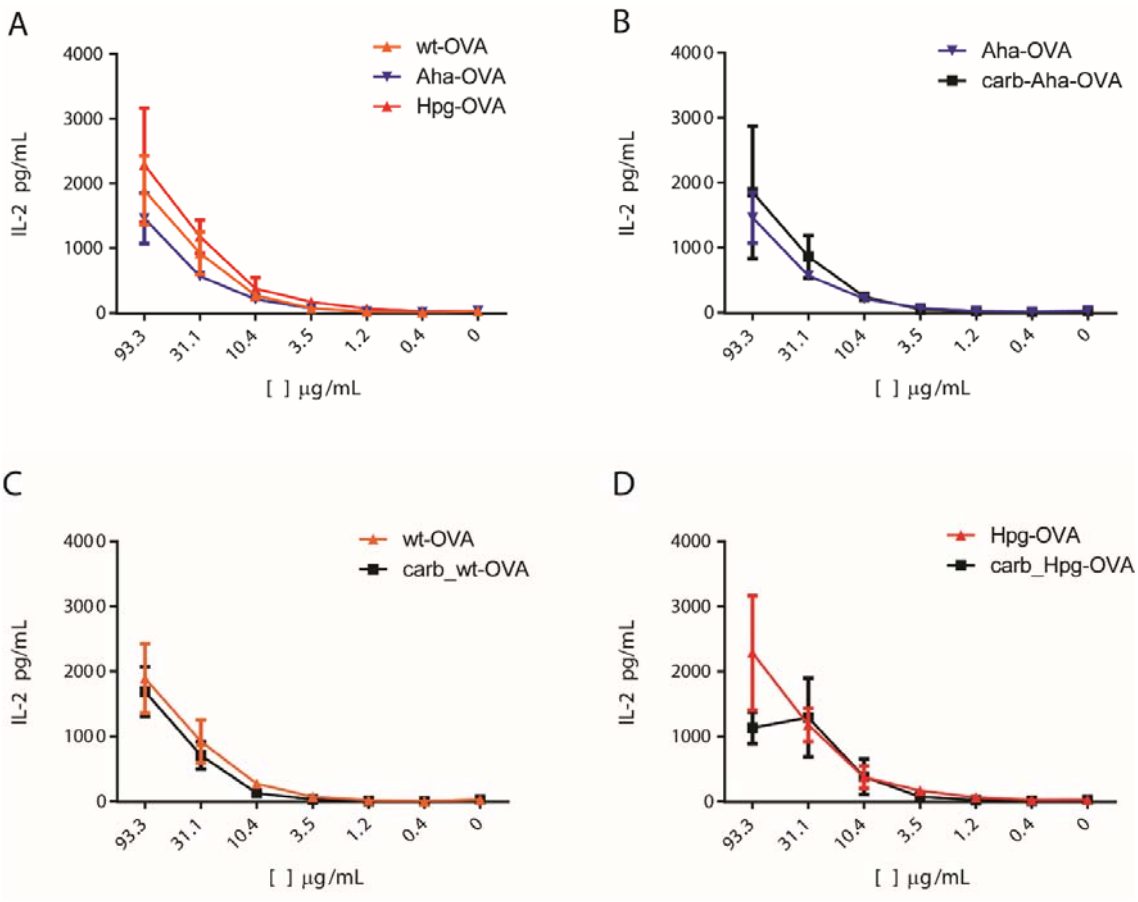

Figure 5: ***Influence of carbamylation of Ovalbumin on the activation of antigen specific CD4^{+} T-cells and cytokine levels.*** A: ELISA (IL-2) read out for CD4+ T-cell proliferation after feeding BMDCs with non-carbamylated wildtype (orange triangle) and bioorthogonal (blue triangle, Aha-Ova; red triangle Hpg-Ova) antigens. B: IL-2 concentration for Aha-Ova (blue triangles) in comparison with carb_Aha-Ova (black squares). Comparison of IL-2 levels in samples treated with C: wt-Ova (orange triangles), with carb_wt-Ova (black squares), D: Hpg-Ova (red triangles) with carb_Hpg-Ova (black squares). n=3 independent with at least two experimental (N=2) replicates.

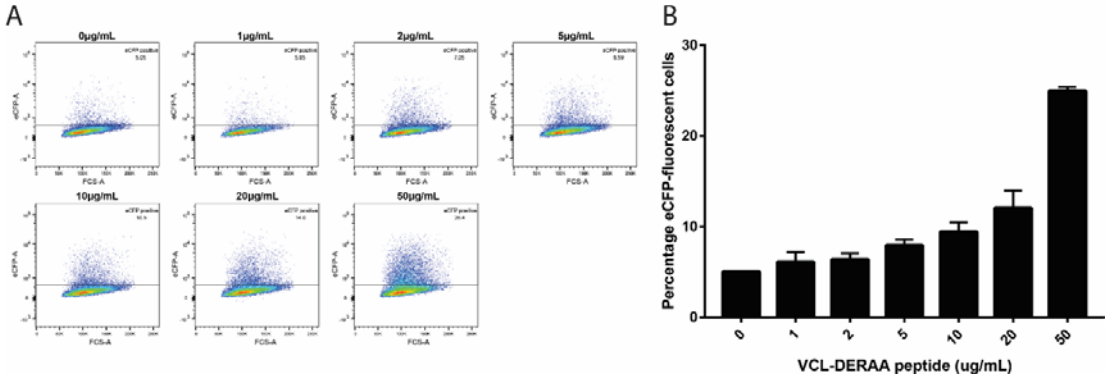

Figure 6: ***T-cell activation of Jurkat-DERAA cells with titrated amounts of VCL-DERAA peptide.***
The T-cells were stimulated by HLA-DQA1*03:01/DQB1*03:02+ (HLA-DQ8+) EBV-transformed B cells presenting VCL-DERAA peptide with titrated amounts (0-50 µg/mL). The TCR on Jurkat-DERAA recognizes VCL-DERAA peptide in a dose-dependent manner. A: eCFP positivity in FACS was used as readout, B: Plotted data in bar graphs, data are shown as n=2 with biological triplicates. Error bars are presented as ±SD.

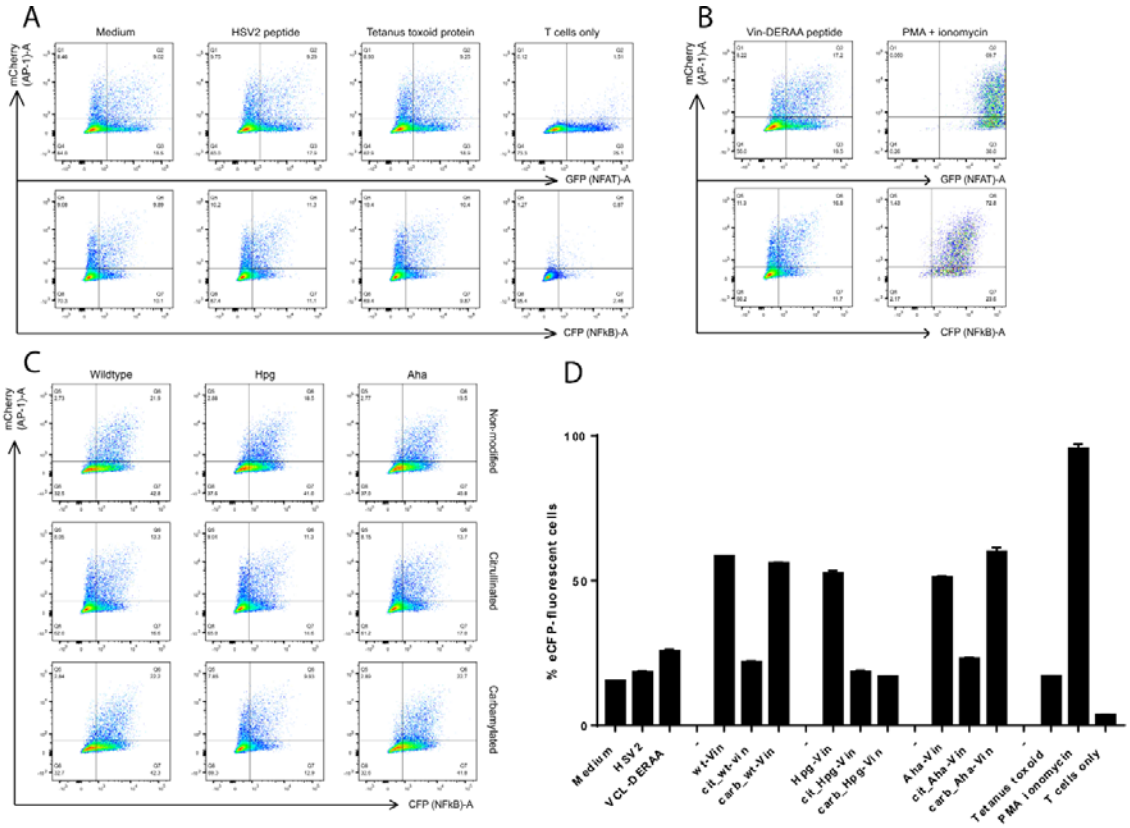

Figure 7: ***T-cell activation assay for carbamylated and citrullinated bioorthogonal Vin variants.***
Dendritic cells pulsed with peptides or Vin variants were cocultured with the Jurkat cells and used for stimulation. Activation of Vin-DERAA-specific Jurkat cells was measured with eCFP expression within the cells. The eCFP expression is dependent on NFkB and is therefore a marker of TCR activation and costimulation, The percentage of live eCFP-positive cells is plotted in bars. HSV2 (Herpes Simplex Virus 2 peptide) and Tetanus toxoid protein are negative controls. VCL-DERAA peptide and PMA-ionomycin are the positive controls. Error bars show the SD. Data is representative of two experiments with biological triplicates.

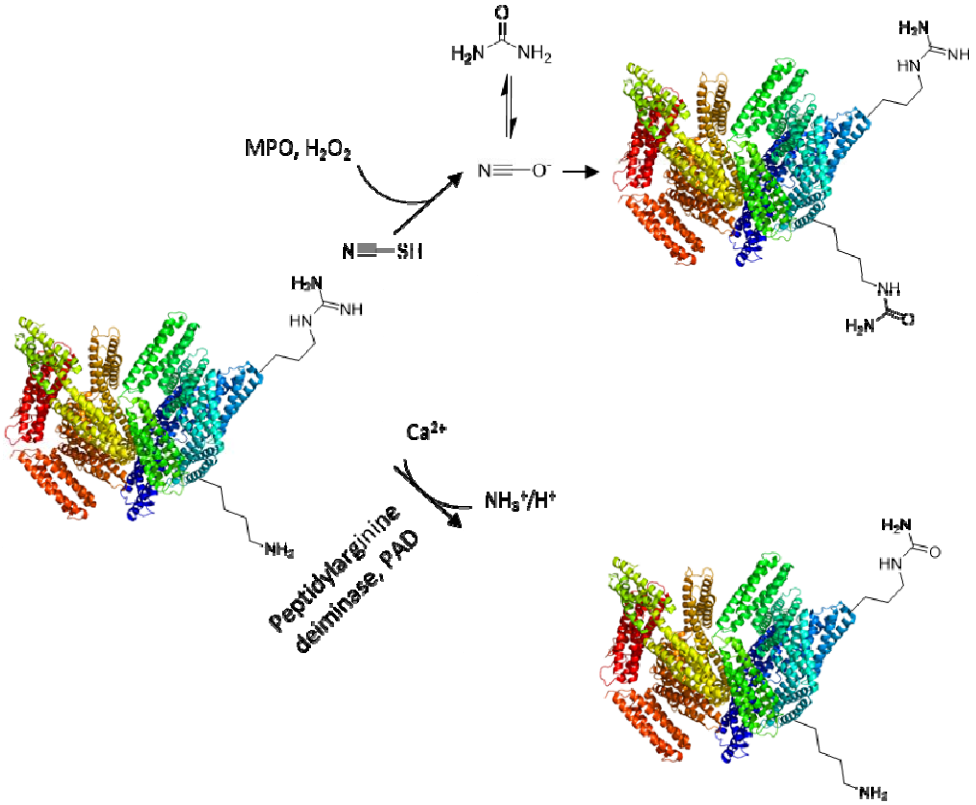

Scheme 1: ***Schematic representation of carbamylation and citrullination of proteins***. Upper panel: carbamylation of primary amines via cyanate, different biochemical pathways (conversion of urea and myelin peroxidase (MPO) mediated conversion, lower panel: citrullination of arginine via peptidyl arginine deiminase (PAD).

Table 1: ***Distribution of different secondary structure elements of carbamylated, citrullinated and/or acetylated Vin and OVA derivatives***

Protein Variant	α-Helix	β-Sheet	β-Turn	Random coil
Carb_Aha-Vin	56.7%	7.1%	12.8%	22.4%
Carb_Hpg-Vin	49.7%	14.6%	11.5%	23.8%
Cit_Aha-Vin	6.1%	52.7%	16.6%	29.0%
Cit-Hpg-Vin	7.8%	21.6%	17.9%	31.9%
Ac-Aha-Vin	10.8%	42.3%	16.9%	35.0%
Ac-Hpg-Vin	25.7%	32.1%	14.6%	29.3%
Carb_Aha-OVA	19.9%	35.0%	16.3%	29.0%
Carb_Hpg-OVA	16.0%	34.5%	16.7%	33.0%
Cit_Aha-OVA	19.7%	35.4%	16.8%	28.7%
Cit_Hpg-OVA	16.0%	35.2%	16.8%	33.0%